STAR Beam Energy Scan Program: Status and Perspectives

Lijuan Ruan (BNL)

February 20, 2023

@BrookhavenLab

GSI Colloquium

RHIC @ Brookhaven National Laboratory

24 years of RHIC operation

The mission of RHIC

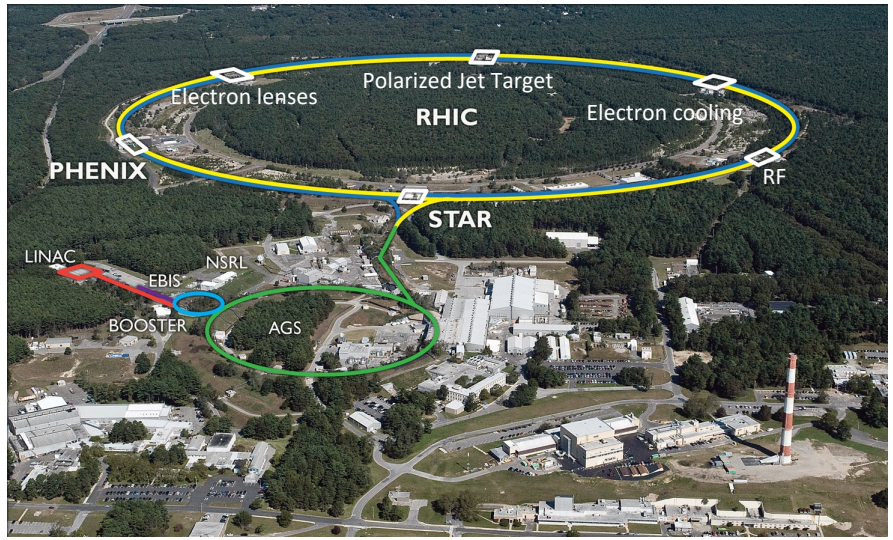

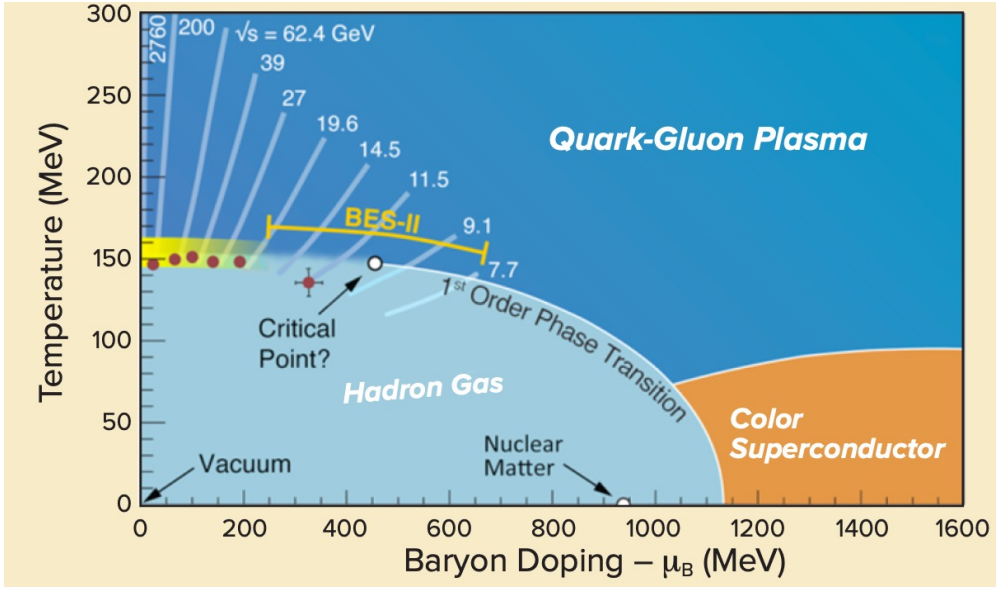

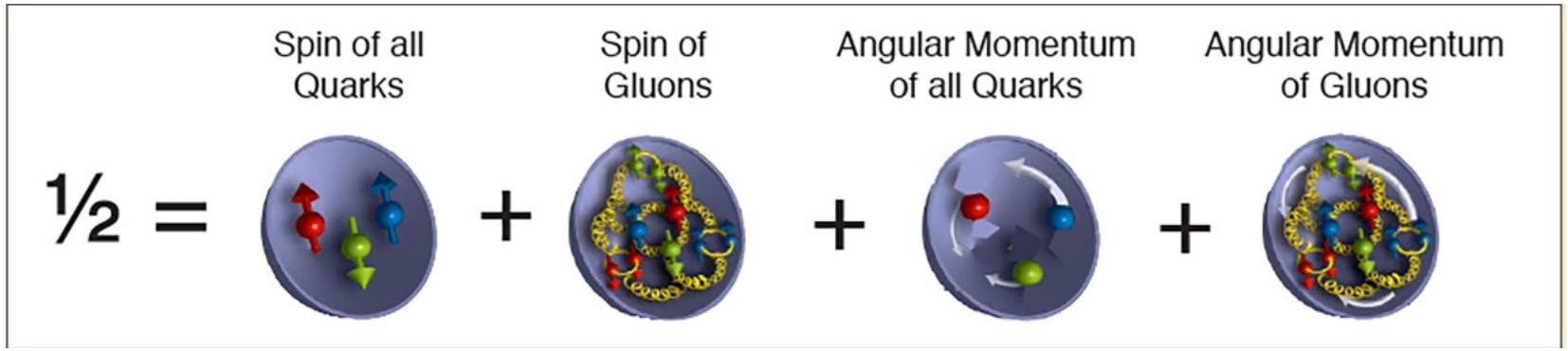

To probe the inner workings of the Quark-Gluon Plasma

To map the phase diagram of QCD

To study the spin puzzle of proton

Perfect Liquid discovery

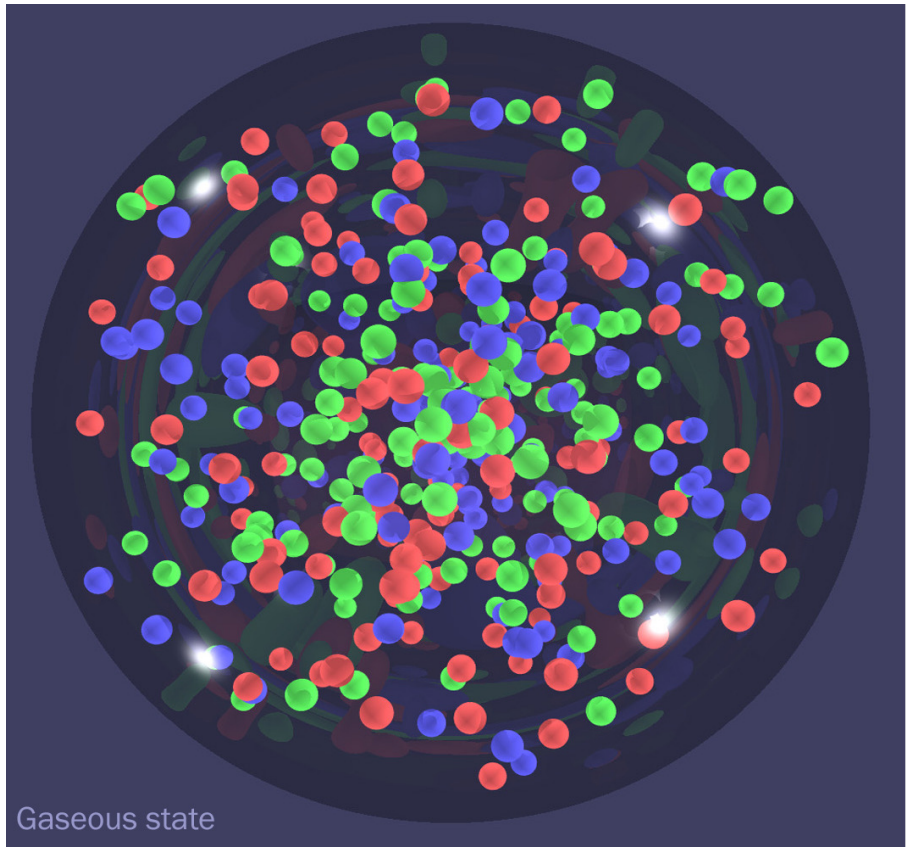

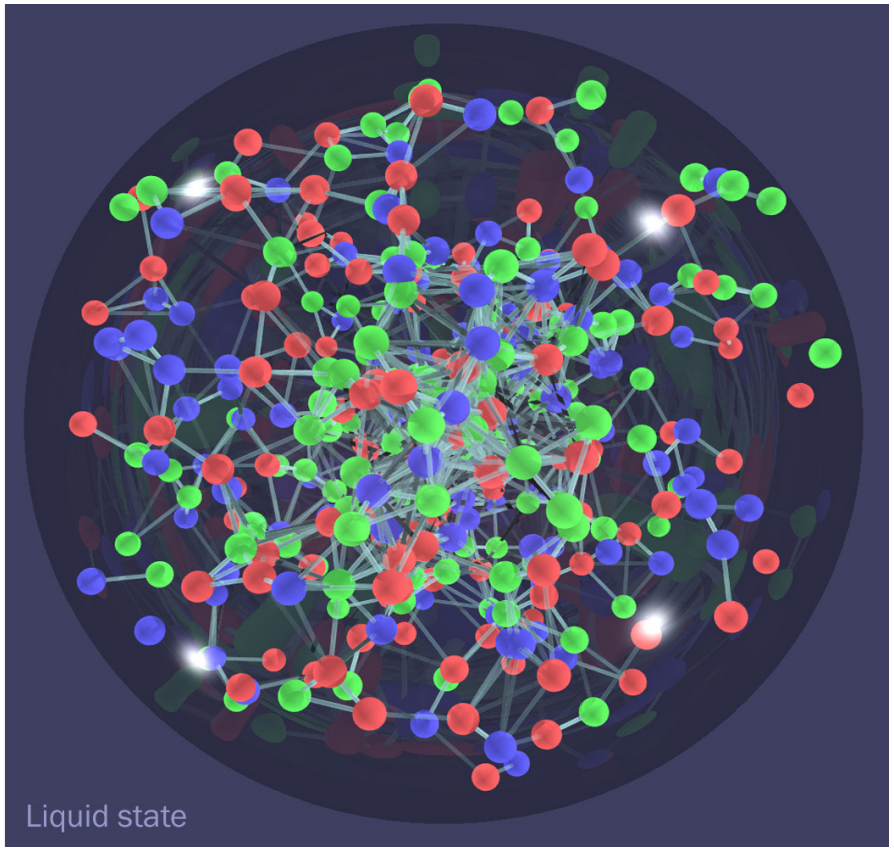

In 2005, BNL announced a discovery of perfect liquid at RHIC

https://www.bnl.gov/newsroom/news.php?a=110303

The properties of perfect liquid

The 2023 NSAC Long Range Plan for Nuclear Science

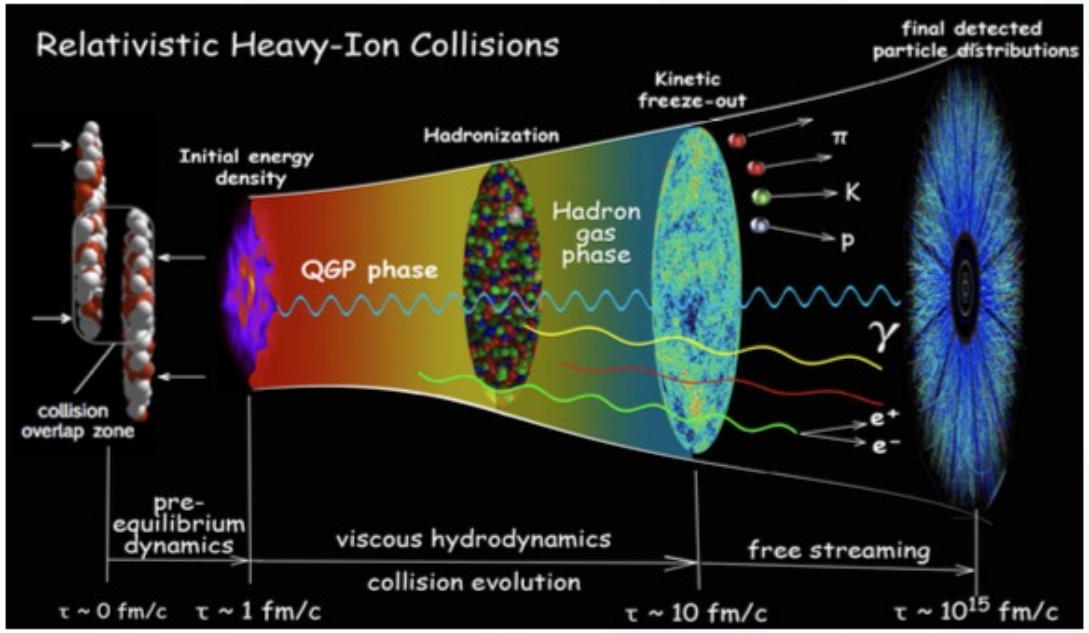

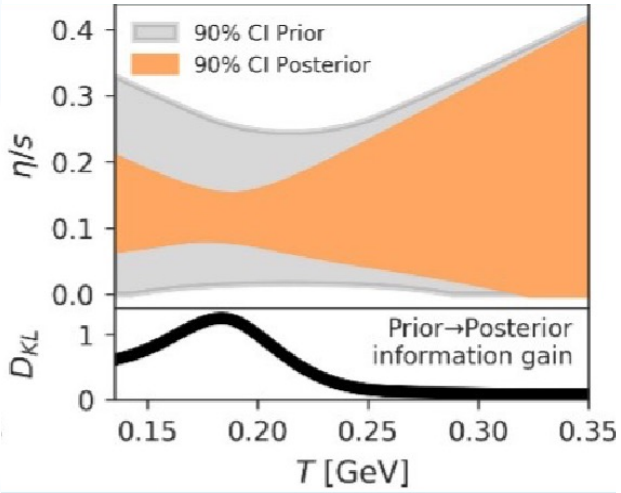

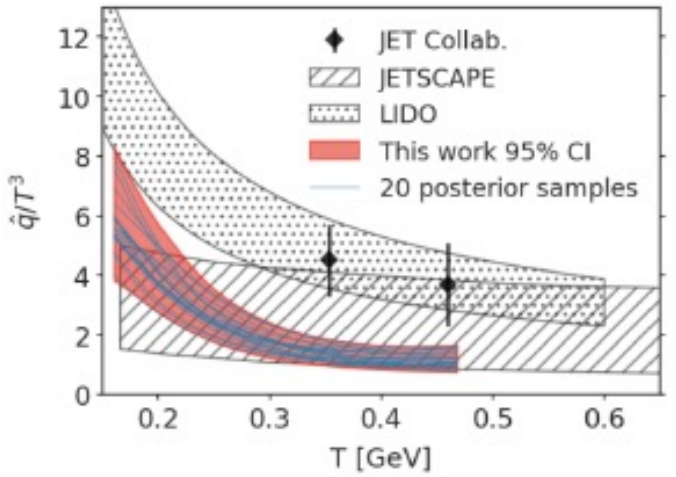

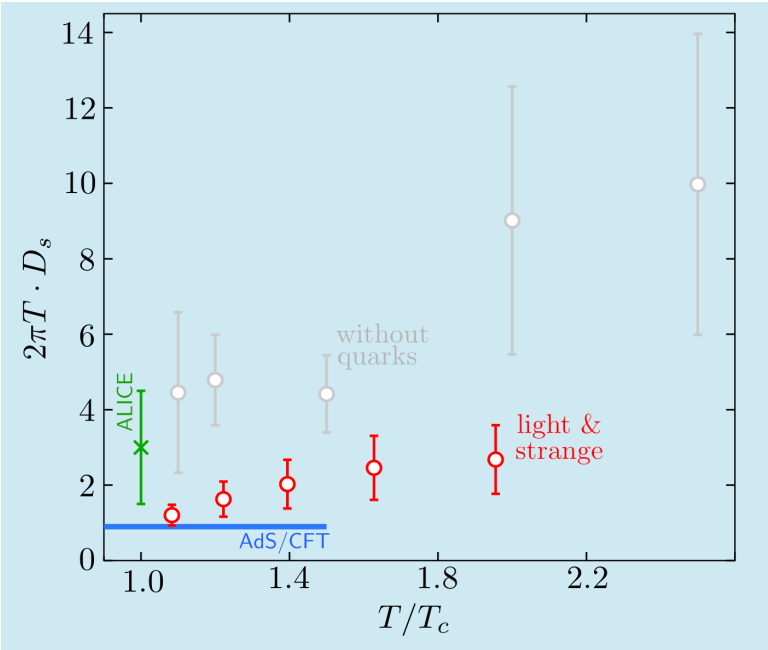

Essential questions to be addressed:

1. How do the fundamental interactions between quarks and gluons lead to the perfect fluid behavior of the quark-gluon plasma?
2. What are the limits on the fluid behavior of matter?
3. What are the properties of QCD matter?
4. What is the correct phase diagram of nuclear matter?

The phases of QCD matter

Lattice QCD: crossover chiral transition at $\mu_B < 2$ T

At top RHIC and LHC energies, measurements consistent with a smooth crossover chiral transition

Change T and μ_B by varying the collision energy:

- Search for the critical point
- Search for the first-order phase transition
- Search for the threshold of QGP formation

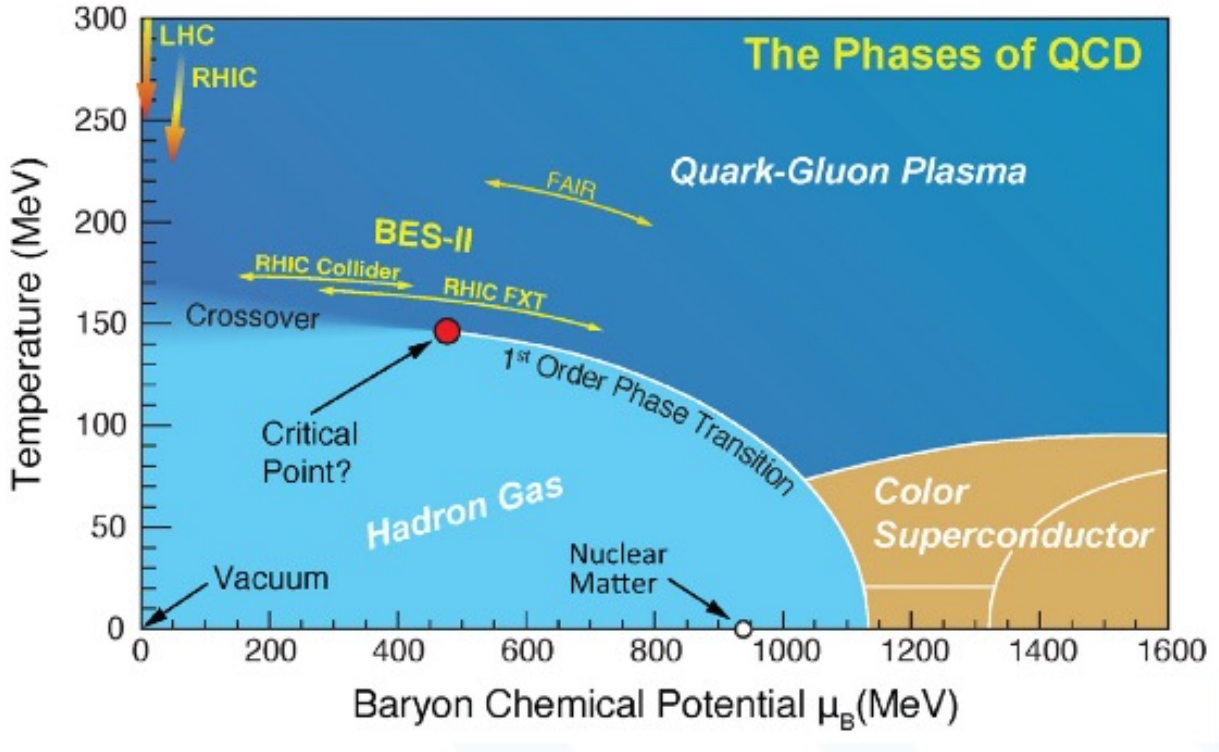

How to infer the QCD critical point

Divergence of the correlation length, dynamics slow down, Large density fluctuations

Critical opalescence, magnetic susceptibility

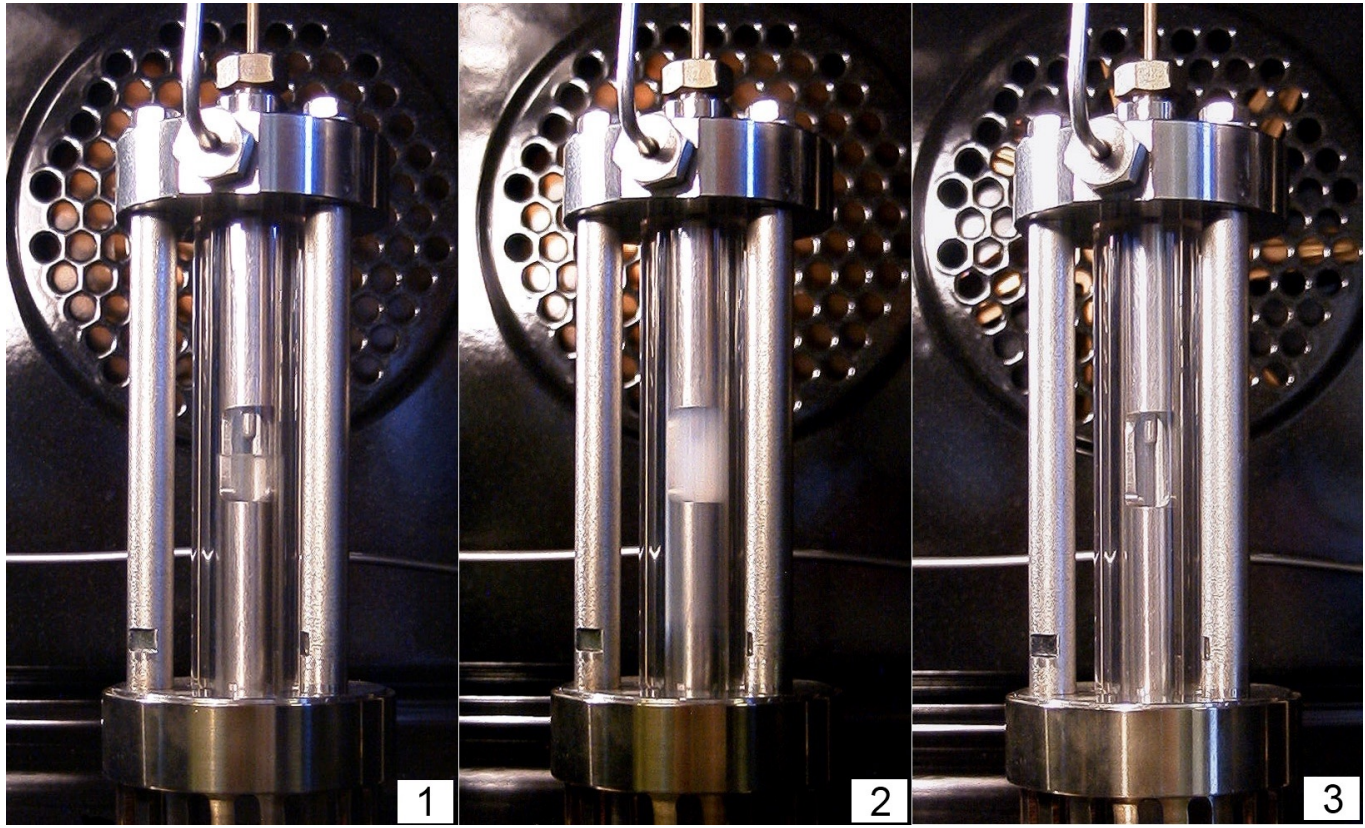

How to infer the QCD critical point

Correlation length related to various moments of the distributions of conserved quantities such as net-baryon, net-charge, and net-strangeness.

$$<(\delta N)^2>\approx\xi^2, <(\delta N)^3>\approx\xi^{4.5}, <(\delta N)^4>-3<(\delta N)^2>^2\approx\xi^7$$

Mean: $M=<N>$

St. Deviation: $\sigma=\sqrt{<(N-<N>)^2>}$

Skewness: $S=\dfrac{<(N-<N>)^3>}{\sigma^3}$

Kurtosis: $\kappa=\dfrac{<(N-<N>)^4>}{\sigma^4}-3$

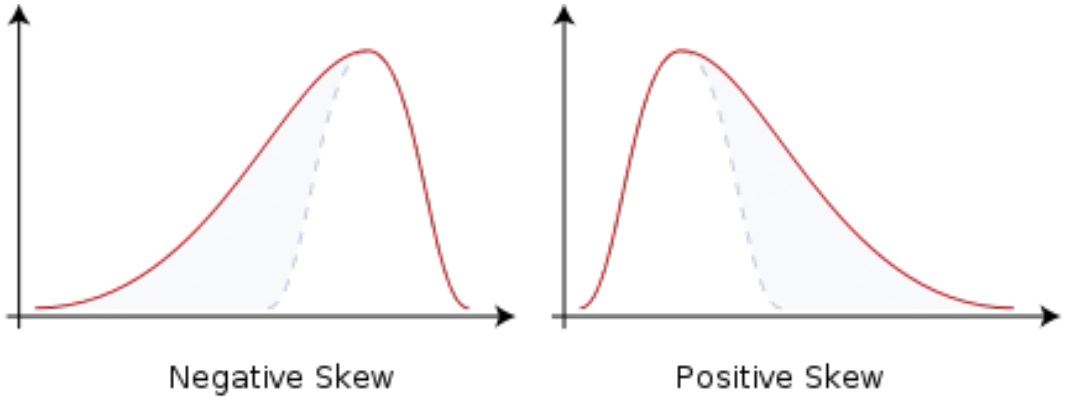

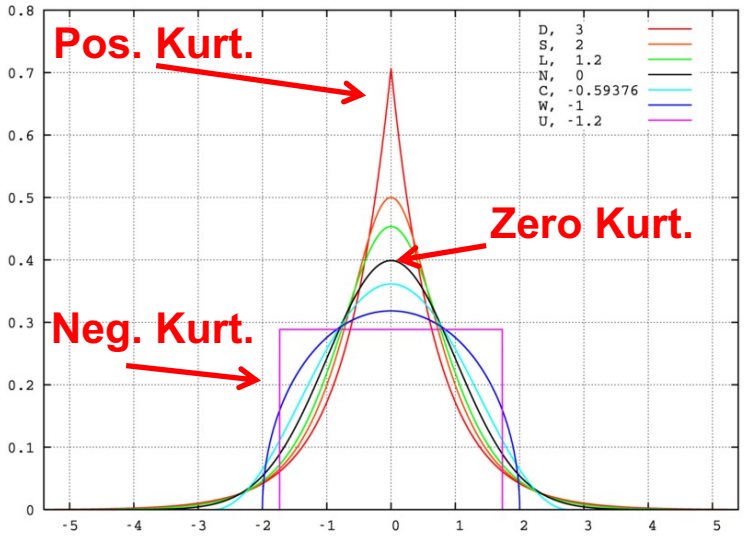

Measure non-Gaussian fluctuation of conserved quantities

Connection to Lattice QCD

Lattice calculations show that moments of the conserved charge (net-baryon, net-charge, net-strangeness) distributions are related to the susceptibilities

Pressure:

$$\frac{p}{T^4} = \frac{1}{VT^3}\ln Z(V,T,\mu_B,\mu_Q,\mu_S)$$

Susceptibility:

$$\chi_q^{(n)} = \frac{1}{T^4}\frac{\partial^n}{\partial(\mu_q/T)^n}P\left(\frac{T}{T_C},\frac{\mu_q}{T}\right)\Big|_{T/T_C},$$

$q = B,Q,S$ **(Conserved Quantum Number)**

$$\chi_q^{(1)} = \frac{1}{VT^3}\langle\delta N_q\rangle, \chi_q^{(2)} = \frac{1}{VT^3}\left\langle(\delta N_q)^2\right\rangle$$

$$\chi_q^{(3)} = \frac{1}{VT^3}\left\langle(\delta N_q)^3\right\rangle$$

$$\chi_q^{(4)} = \frac{1}{VT^3}\left(\left\langle(\delta N_q)^4\right\rangle - 3\left\langle(\delta N_q)^2\right\rangle^2\right)$$

A. Bazavov et al .*arXiv::1208.1220. 1207.0784.*
F. Karsch et al, PLB 695, 136 (2011).
arXiv: 1203.0784; S. Borsanyi et al, JHEP1201,138(2011);

High moments of net-proton multiplicity distributions

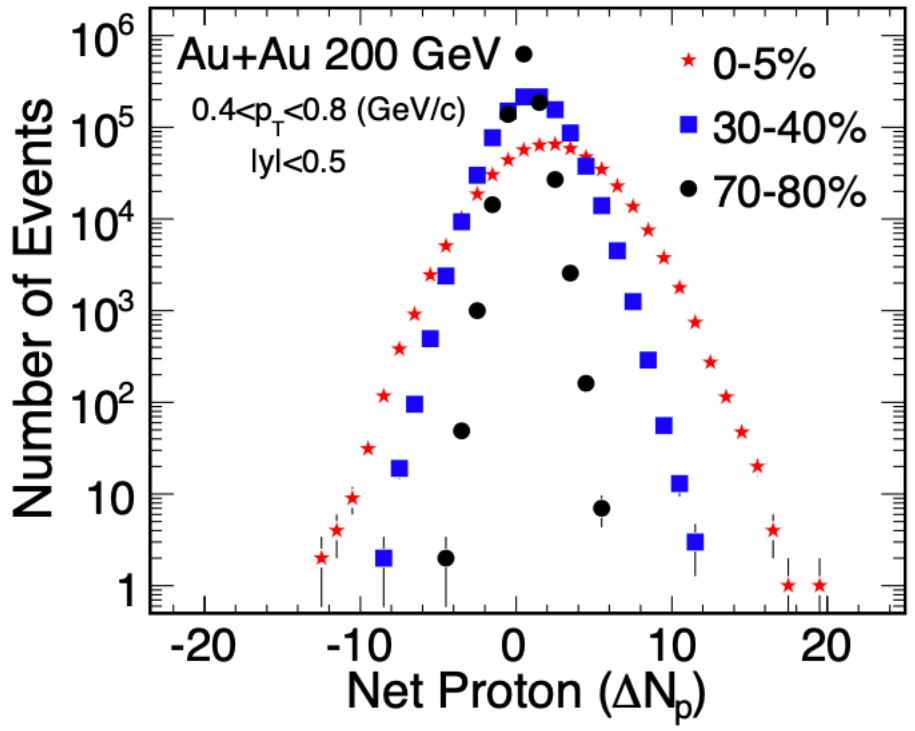

$$\kappa\sigma^2 \sim \frac{\chi^{(4)}}{\chi^{(2)}}, S\sigma \sim \frac{\chi^{(3)}}{\chi^{(2)}}, \frac{\sigma^2}{M} \sim \frac{\chi^{(2)}}{\chi^{(1)}}$$

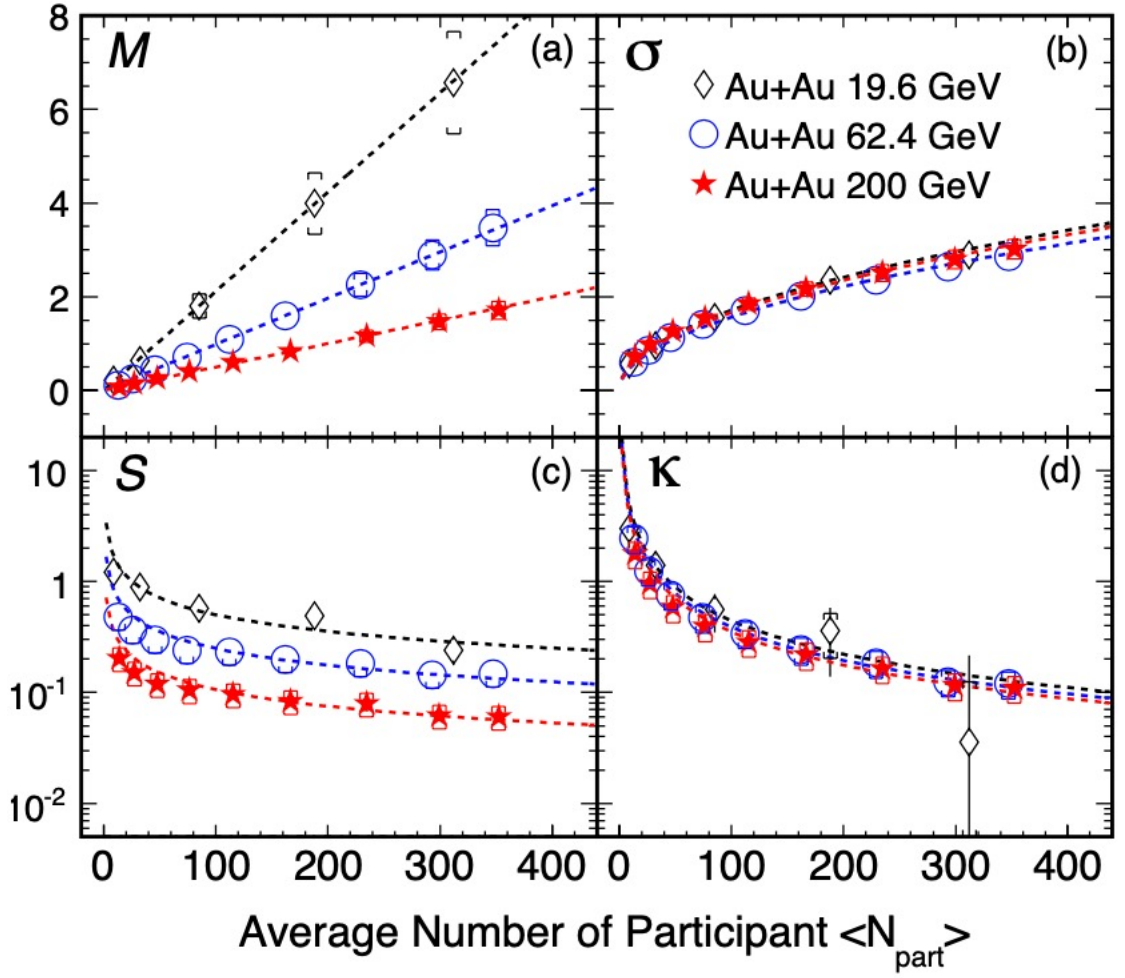

PRL 105 (2010) 022302

High moments of net-proton multiplicity distributions

PRL 105 (2010) 022302

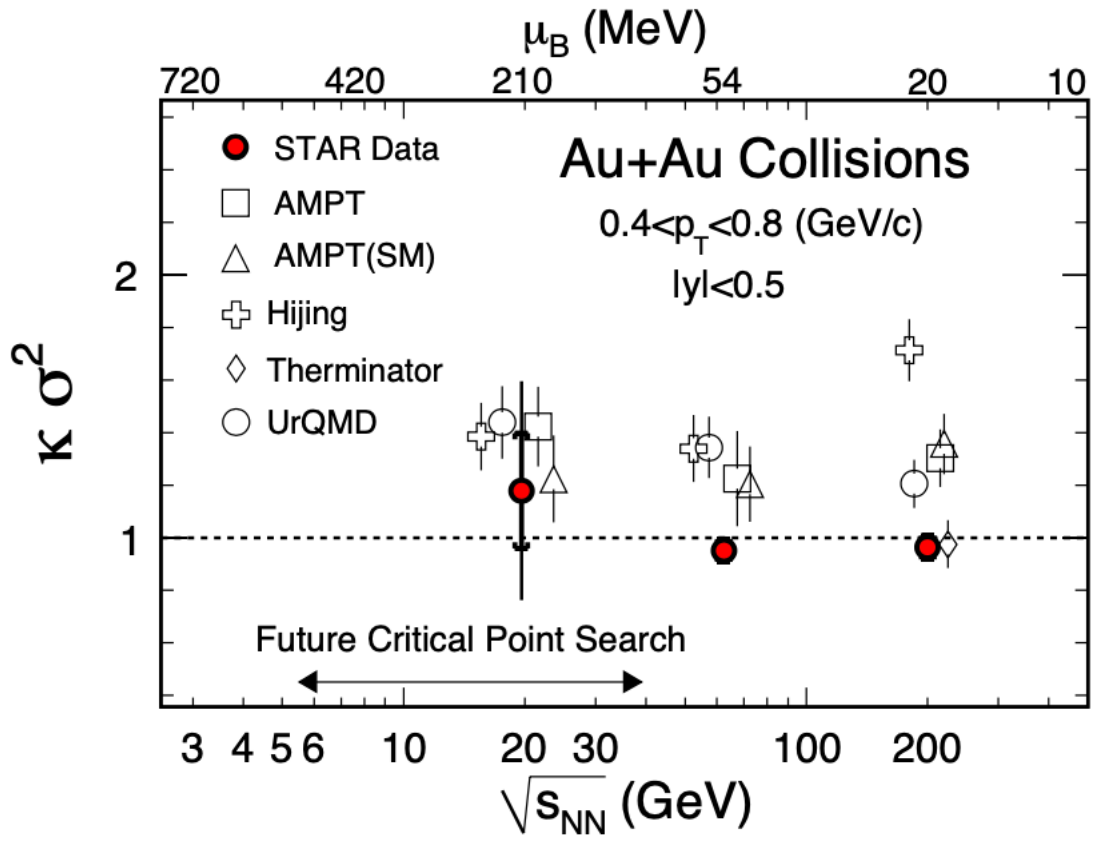

No evidence for a QCD critical point in the QGP phase diagram for **μ_B < 200 MeV**

0.04 M, 5 M, 8 M data used for 19.6, 62.4, and 200 GeV respectively.

STAR beam energy scan phase I campaign

RHIC Multi-Year Beam Use Request
For Run7 – Run 9

The STAR Collaboration

August 24, 2006

In 2006, stated in the Beam Use Request:
definite search for the existence and location of the QCD Critical Point for Run 2009

RHIC Beam Energy Scan Phase I in 2010 and 2011

Energy (GeV)	7.7	11.5	19.6	27	39	62.4	200
Statistics (Million)	~3	~6.6	~15	~30	~87	~47	~242
Year	2010	2010	2011	2011	2010	2010	2010

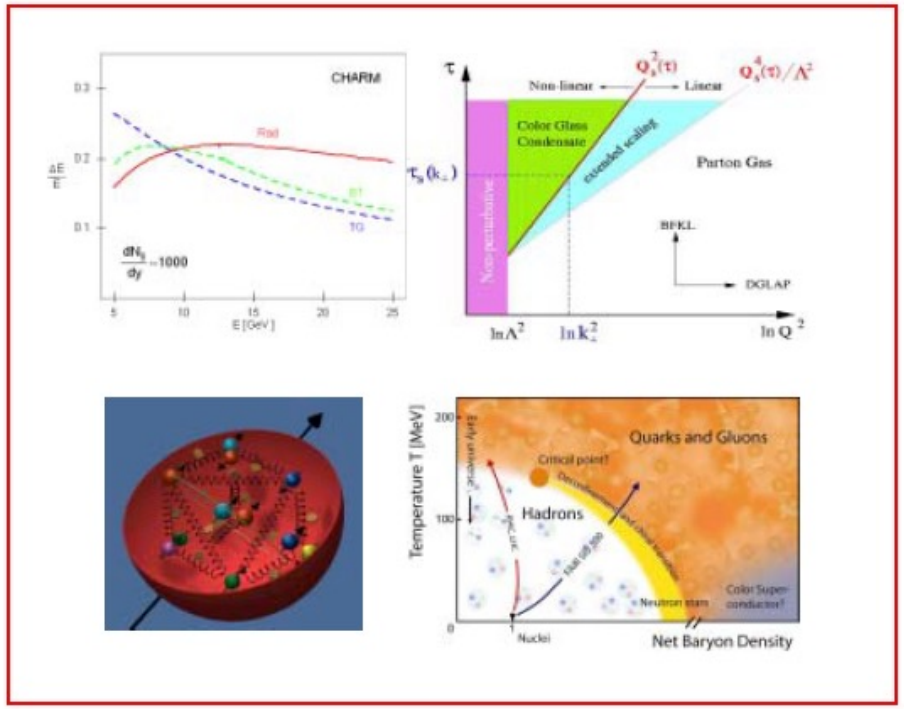

Time of flight detector upgrade just completed before Run 2010

The STAR detector in 2010 and 2011

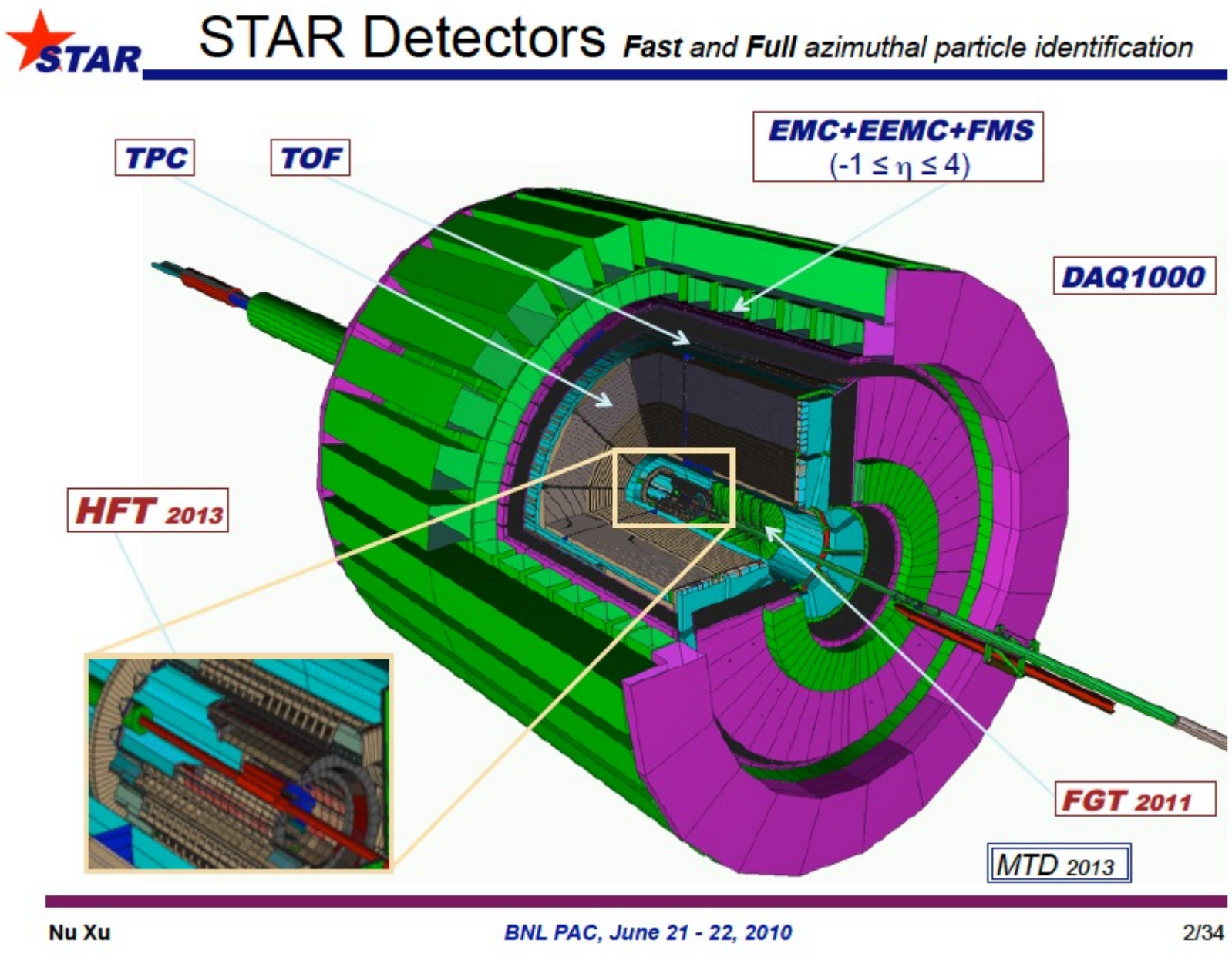

Particle identification with TPC+TOF

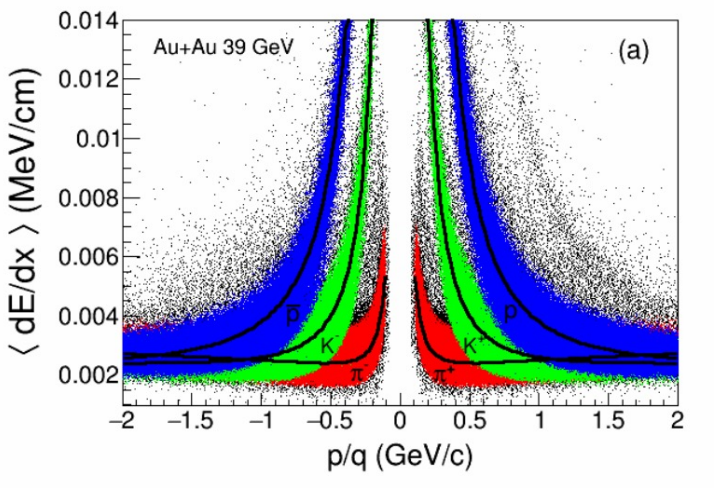

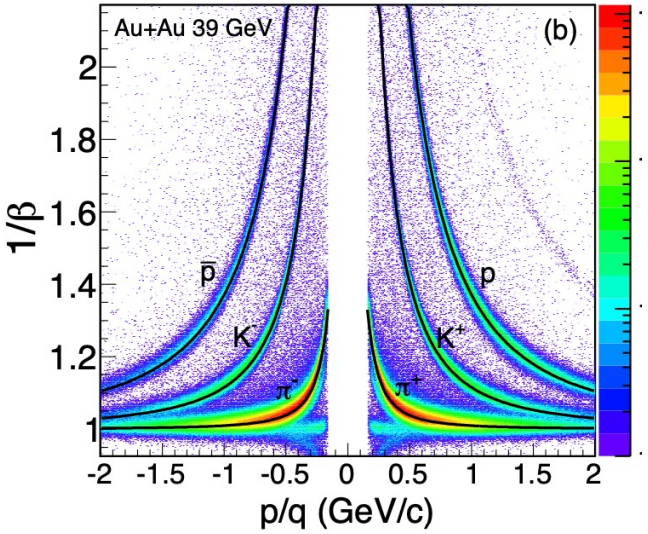

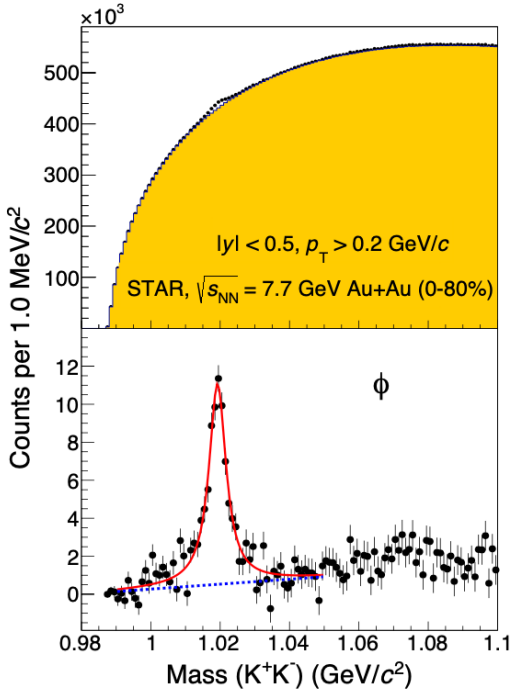

STAR, $\sqrt{s_{NN}}$ = 7.7 GeV Au+Au (0-80%), |y|<0.5

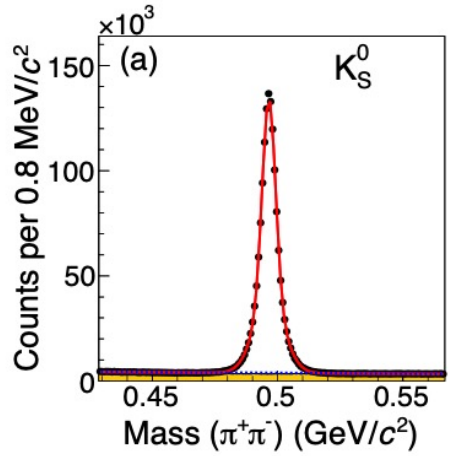

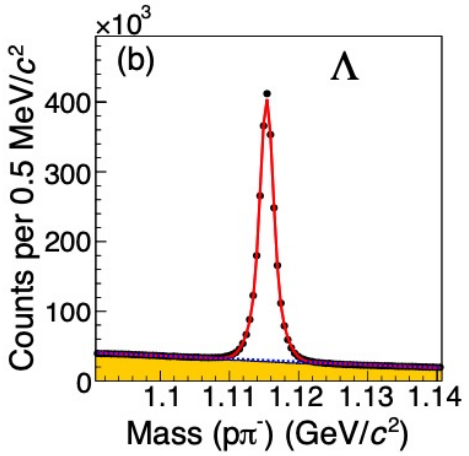

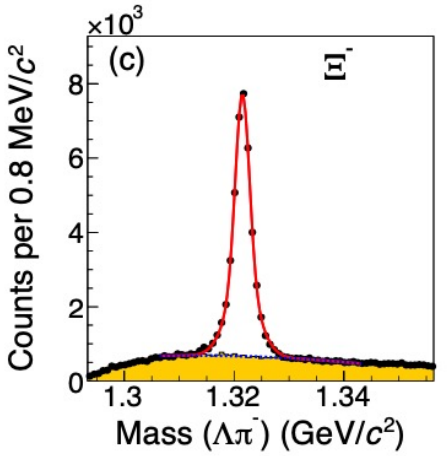

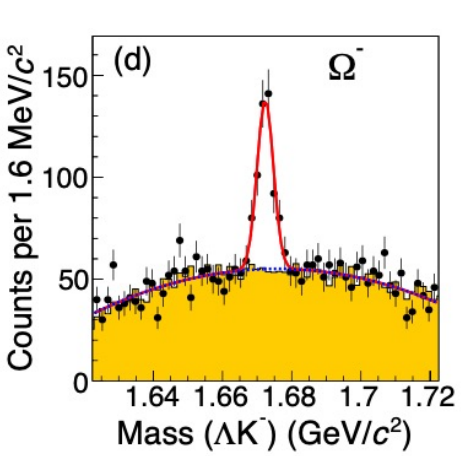

Measure T and μ_B

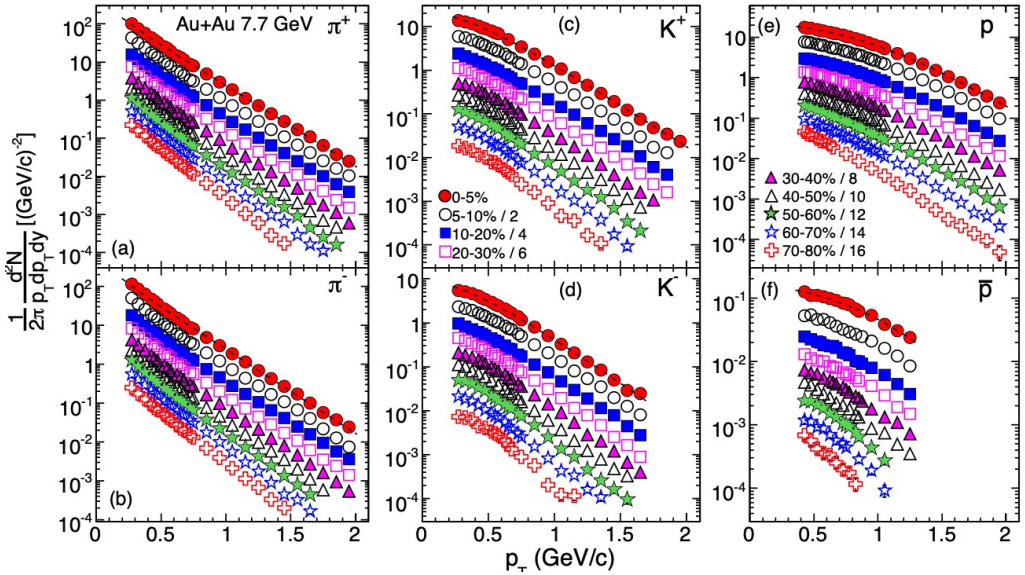

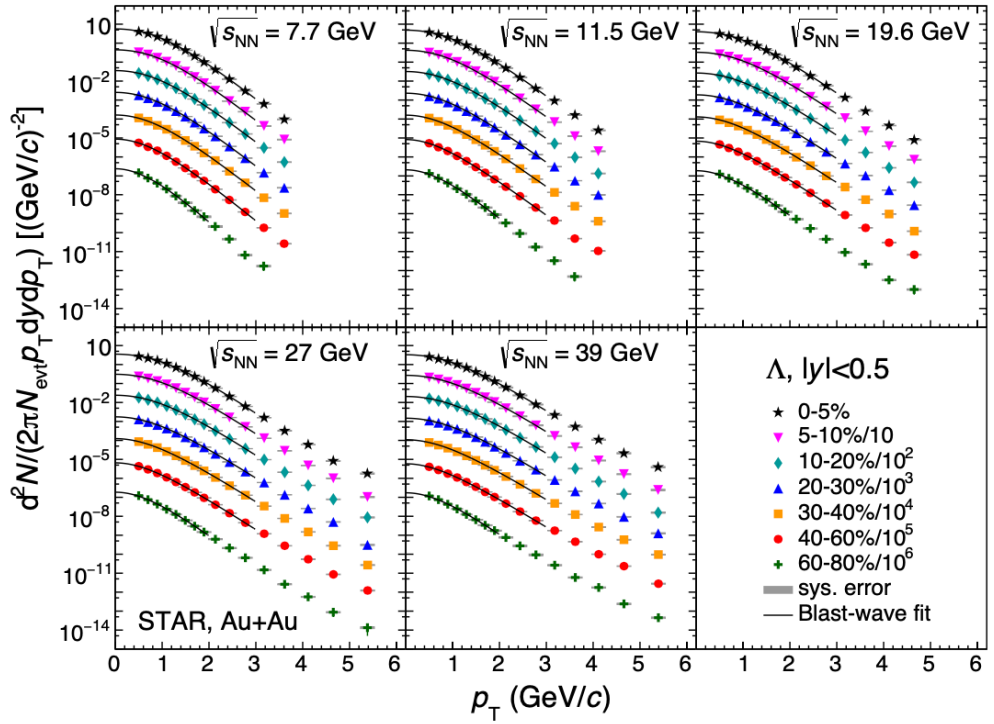

Phys. Rev. C 96 (2017) 44904

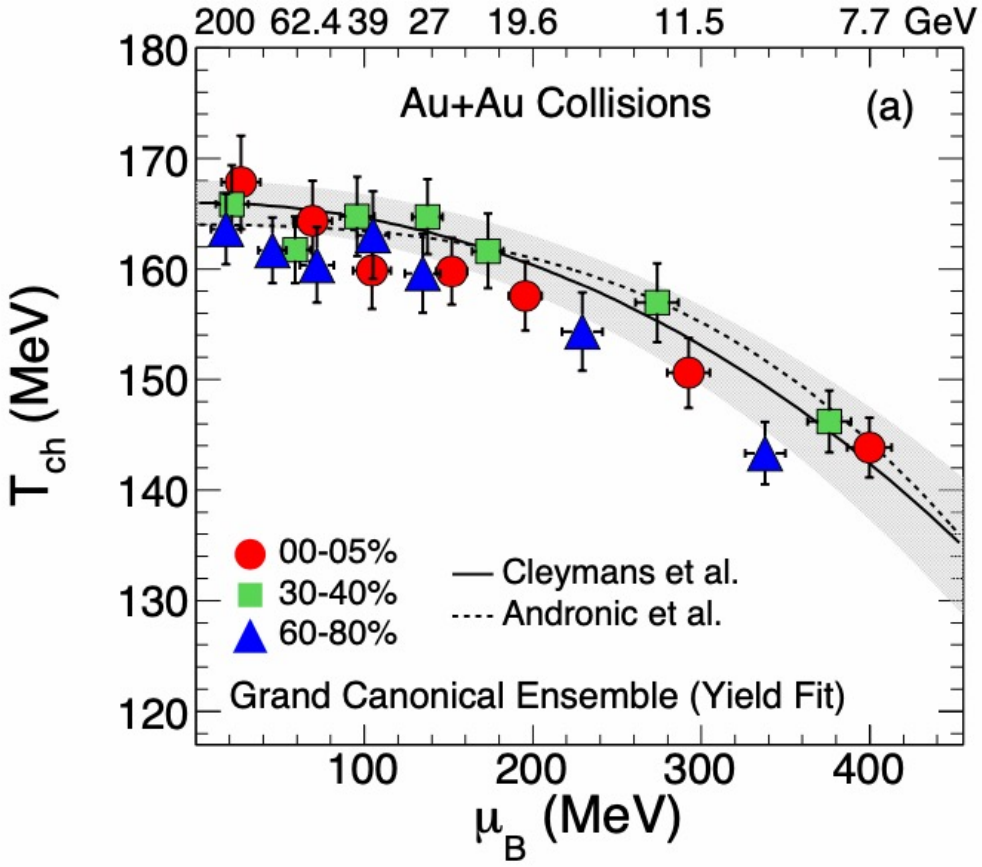

$\pi^{\pm}$, $K^{\pm}$, p, $\bar{p}$, Λ, $\bar{\Lambda}$, Ξ, and $\bar{\Xi}$.

π^-/π^+, $\bar{K}^-/K^+$, $\bar{p}/p$, $\bar{\Lambda}/\Lambda$, $\bar{\Xi}/\Xi$, K^-/π^-, $\bar{p}/\pi^-$, Λ/π^-, and $\bar{\Xi}/\pi^-$.

Photons and dileptons

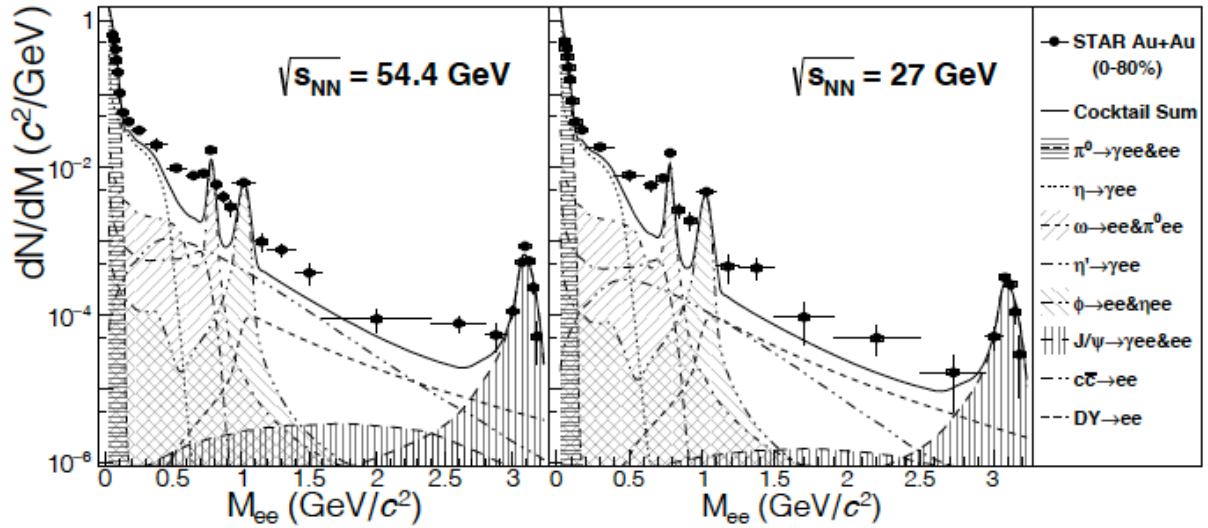

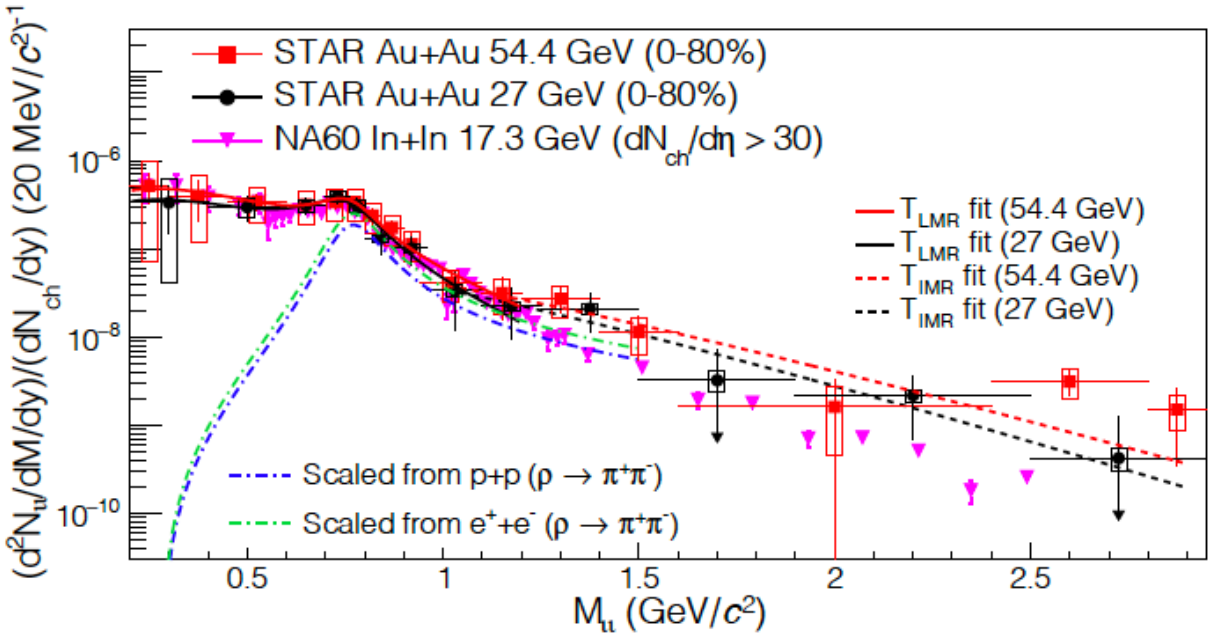

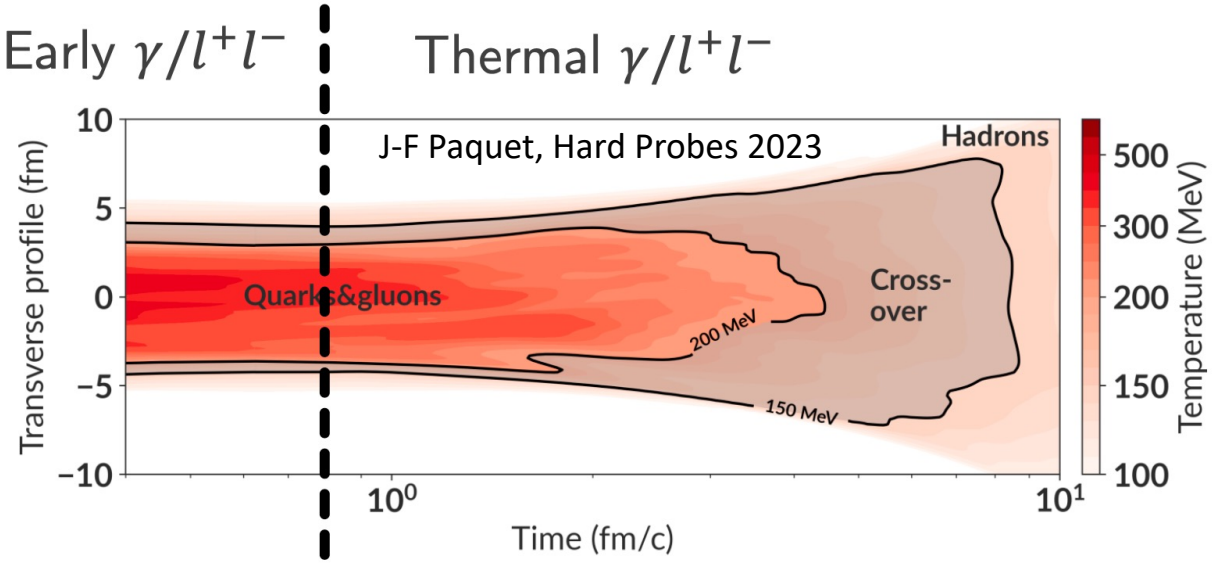

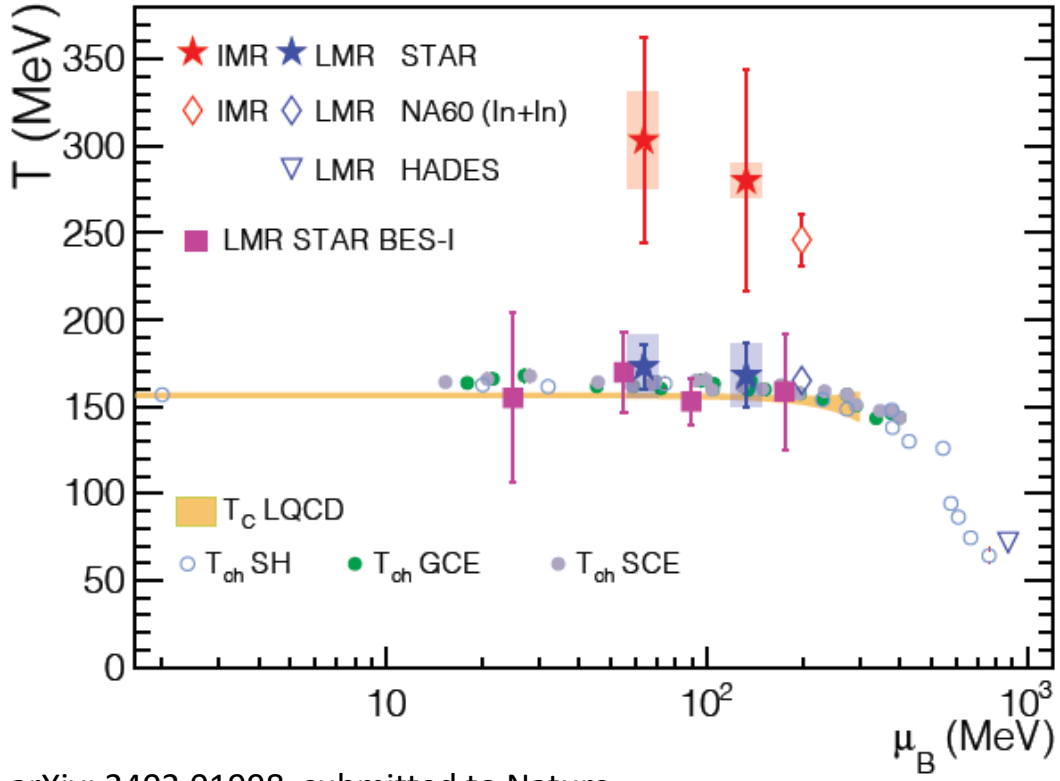

arXiv: 2402.01998, submitted to Nature

Net-proton higher moments from BES-I with TOF

PRL 126 (2021) 92301

$20 < \mu_B < 420$ MeV

pT range extended to 0.4-2 GeV/c

14.5 and 54.4 GeV data included

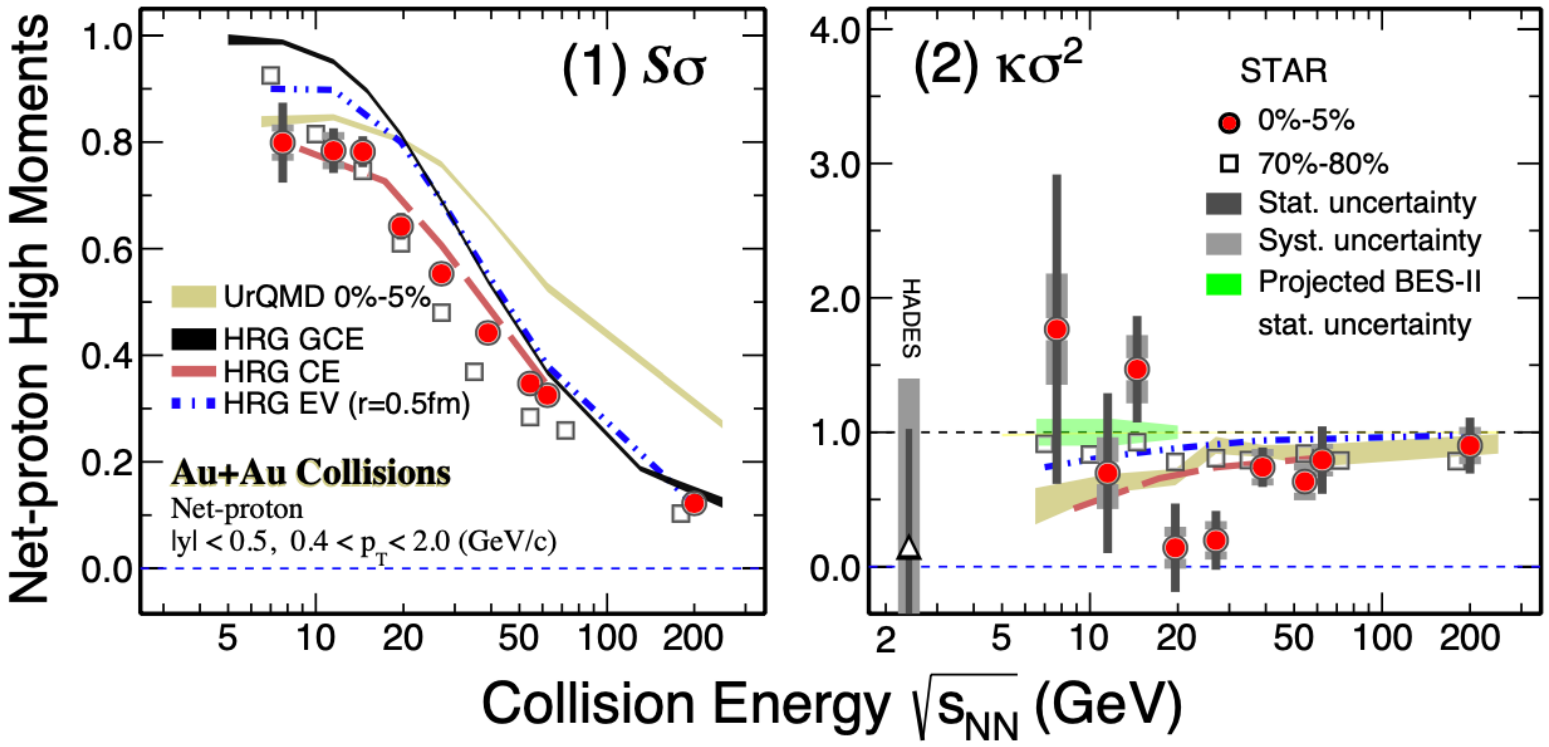

First evidence of a non-monotonic variation in kurtosis times variance of the net-proton number distribution as a function of collision energy with 3.1 sigma significance

Light nuclei yield ratio

PRL 130 (2023) 202301

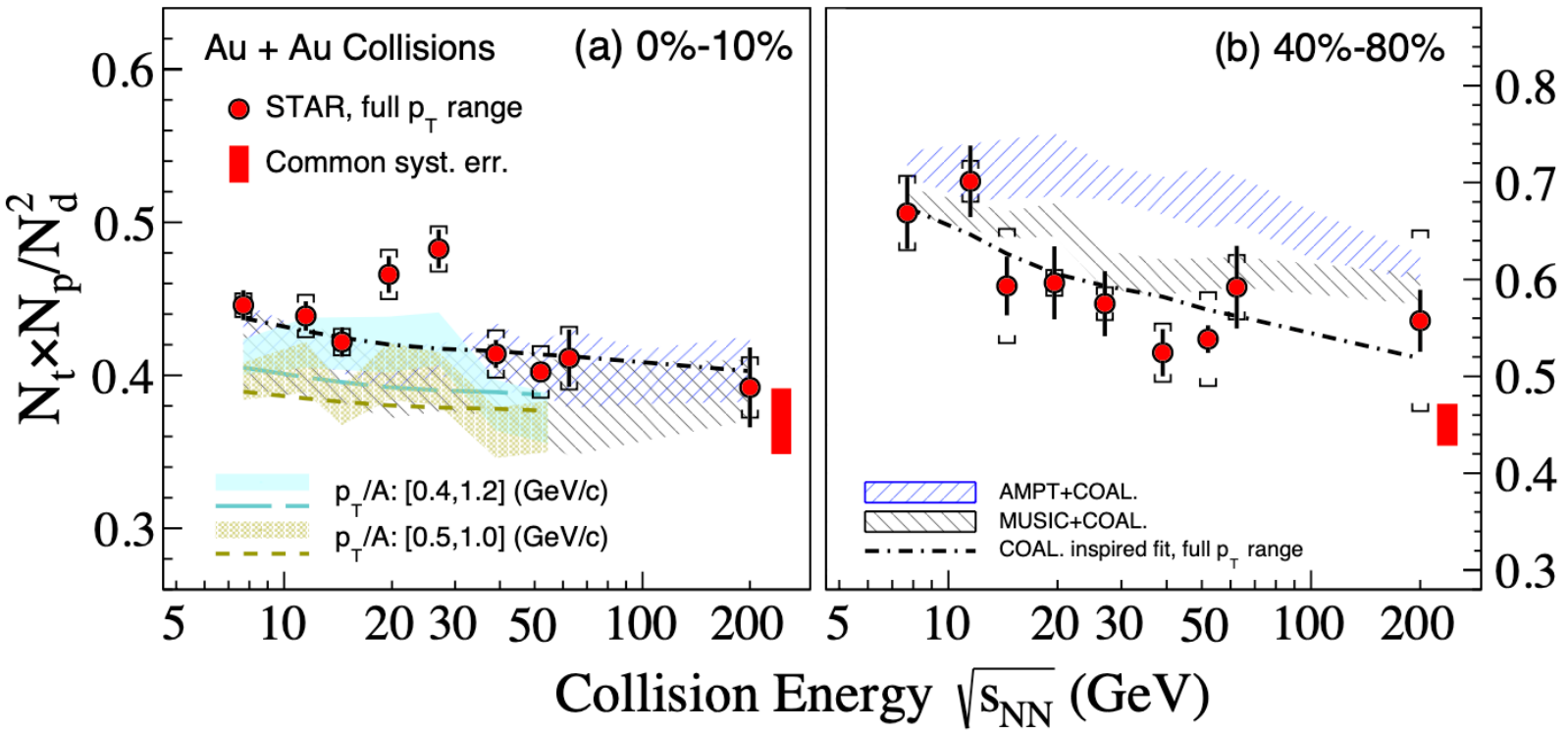

N_tN_p/N_d^2, sensitive to fluctuations of the local neutron density shows enhancements relative to the coalescence baseline with a significance of 2.3σ and 3.4σ respectively in 0 –10% central Au+Au collisions at 19.6 and 27 GeV.

Constrain production dynamics of light nuclei and understanding of the QCD phase diagram

Beam energy dependence of identified particle v_1 slope

Directed flow: first harmonic in the Fourier expansion of the azimuthal distribution of produced particles with respect to the reaction plane

$$\frac{dN}{d(\phi - \Psi_{RP})} = k\{1 + \sum_{n=1}^{\infty} 2v_n \cos[n(\phi - \Psi_{RP})]\}$$

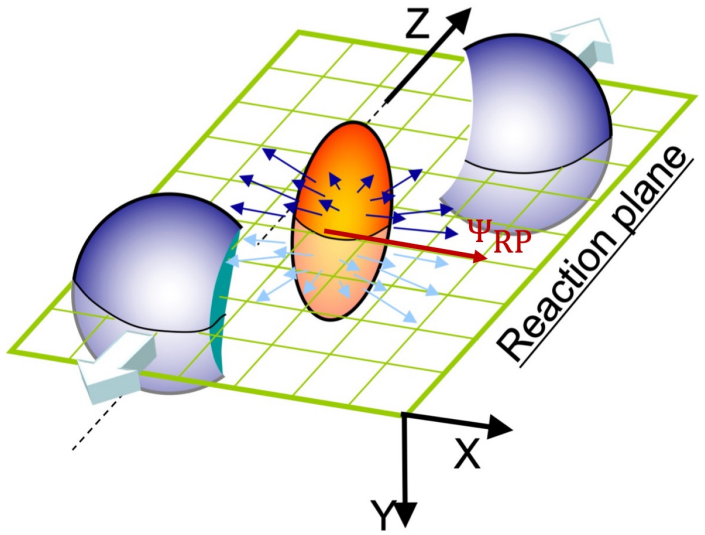

Describes collective sideward motion of produced particles and nuclear fragments and carries information on the very early stages of the collision

A.M. Poskanzer and S.A. Voloshin, Phys. Rev. C 58, 1671(1998)

Phys. Rev. Lett. **120** (2018) 62301
Phys. Rev. Lett. **112** (2014) 162301

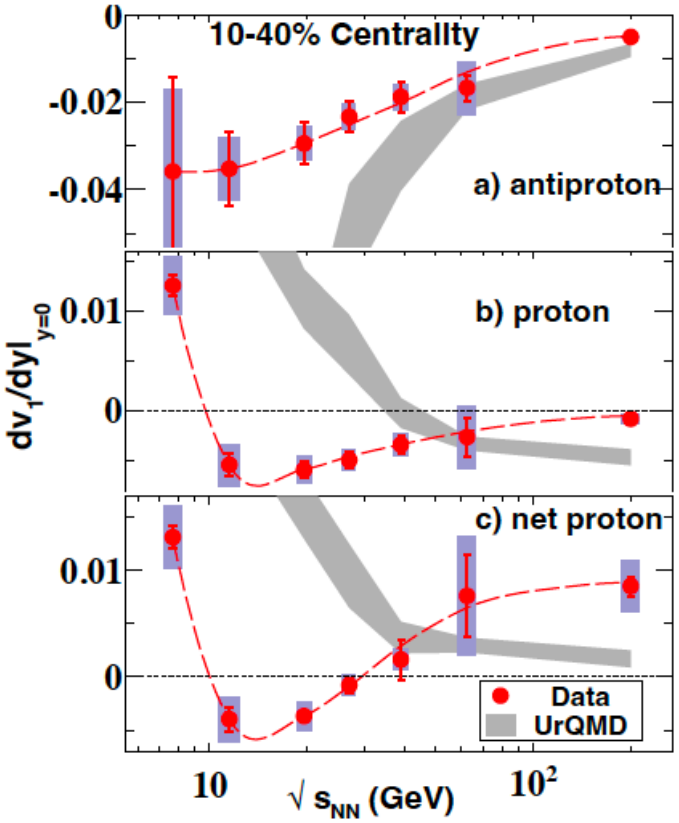

v_1 slope near midrapidity for pions and antiprotons is negative

Proton slope changes sign

Net-proton slope changes sign twice

Vorticity of multi-strange hadrons

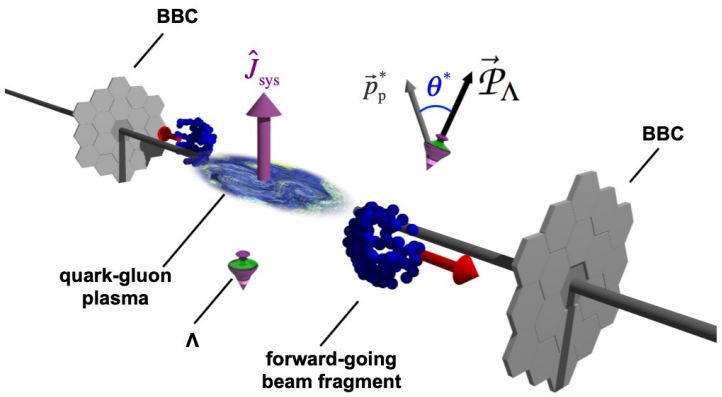

Global angular momentum transfer to hyperon polarization

Heavy ion collisions created the most vortical system ever observed.

Nature **548** (2017) 62

PRL126 (2021) 162301

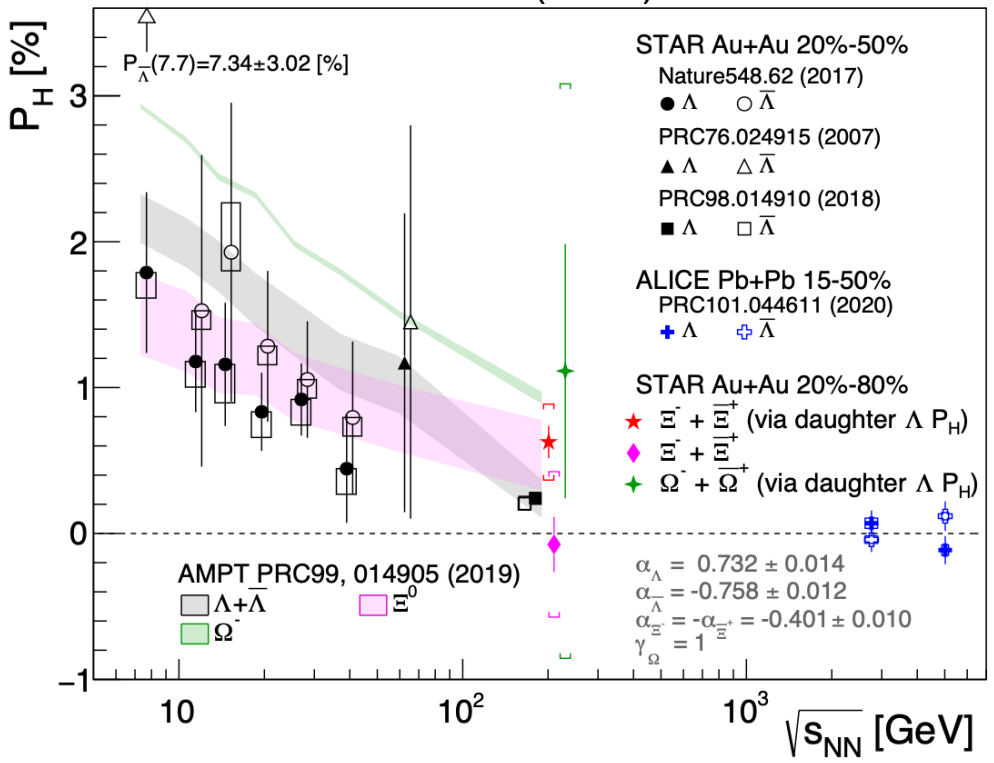

$\langle P_\Lambda \rangle$ (%) = 0.24 ± 0.03 (stat) ± 0.03 (syst)
$\langle P_\Xi \rangle$ (%) = 0.47 ± 0.10 (stat) ± 0.23 (syst)
$\langle P_\Omega \rangle$ (%) = 1.11 ± 0.87 (stat) ± 1.97 (syst)

First measurement of global polarization of Ξ and Ω

Results reinforce picture of system fluid vorticity

STAR beam energy scan phase II campaign

STAR Collaboration Decadal Plan
December 2010

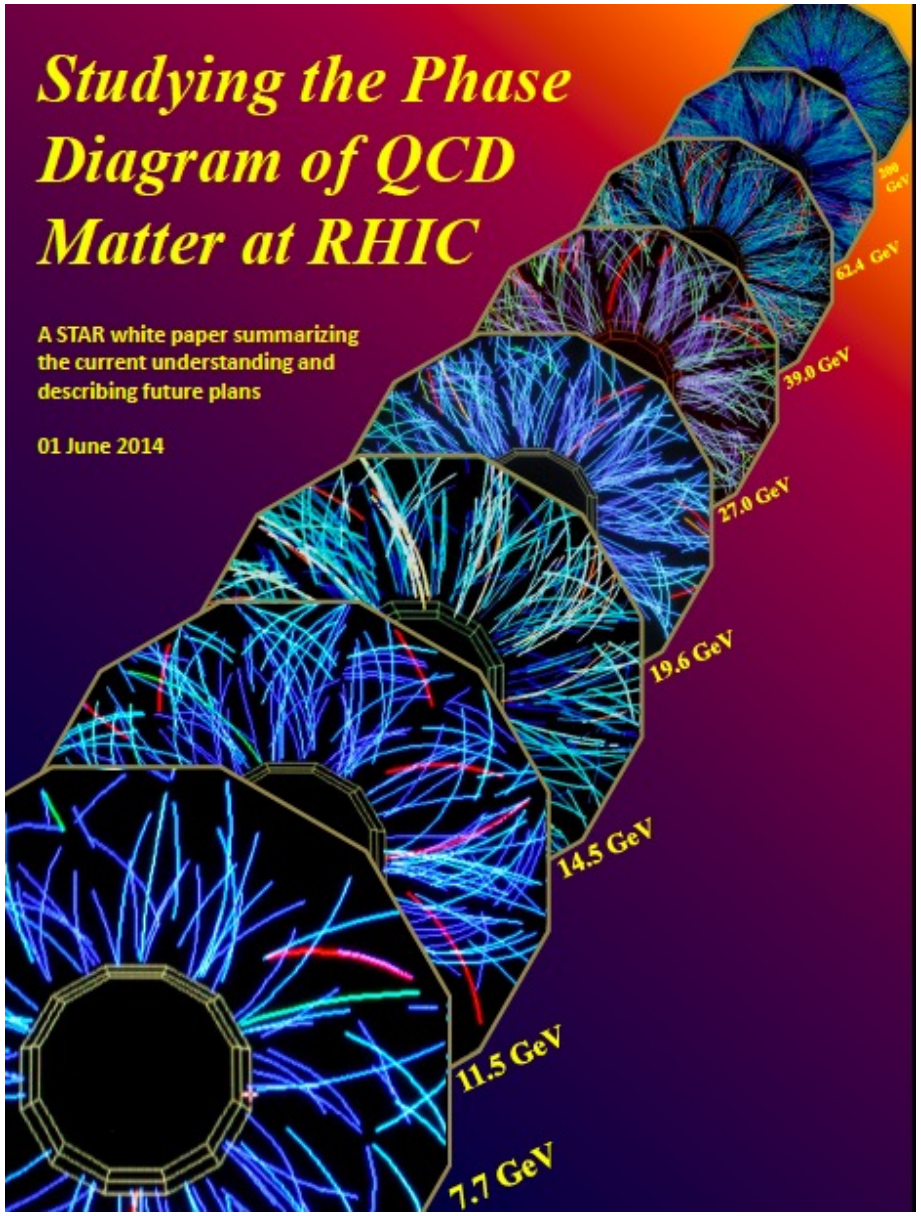

https://drupal.star.bnl.gov/STAR/starnotes/public/sn0598

STAR as a fixed-target experiment

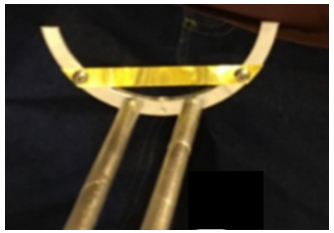

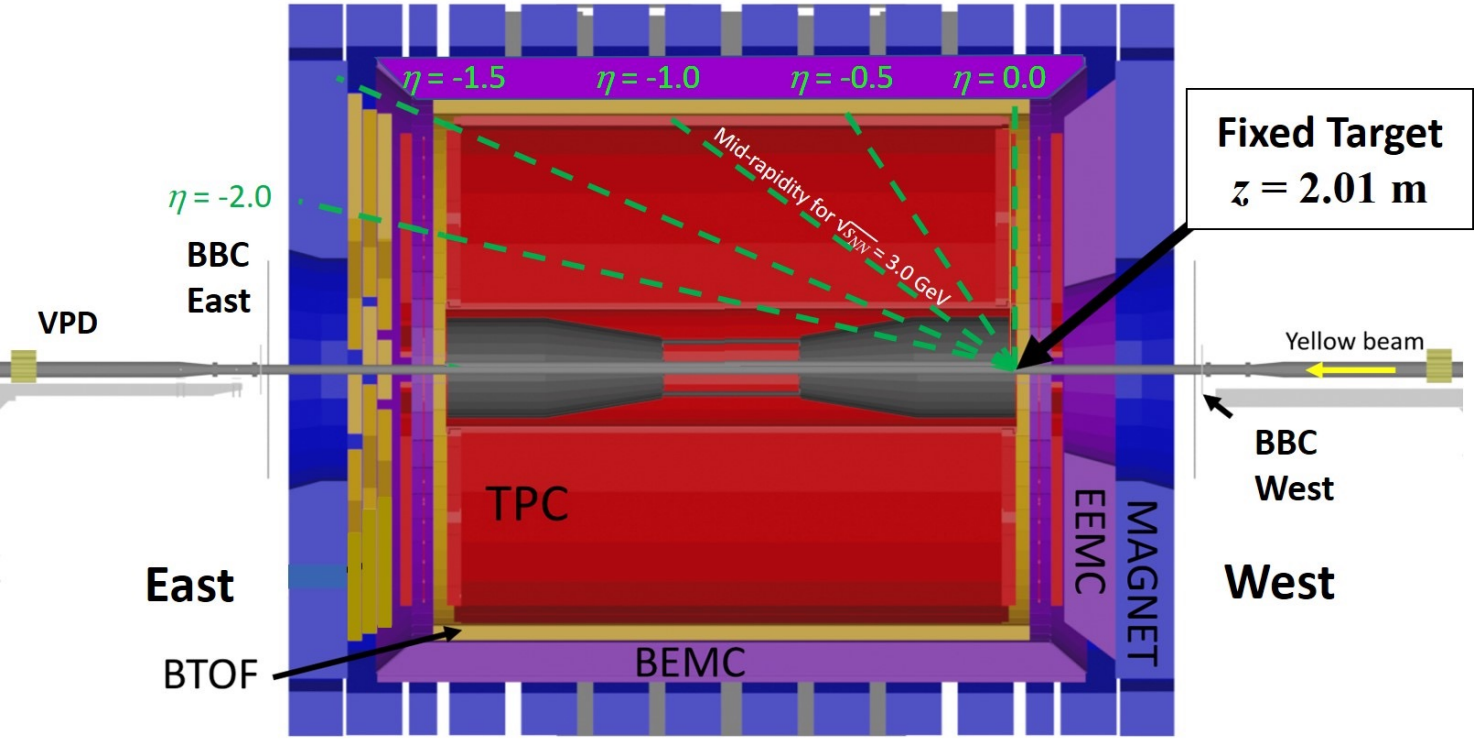

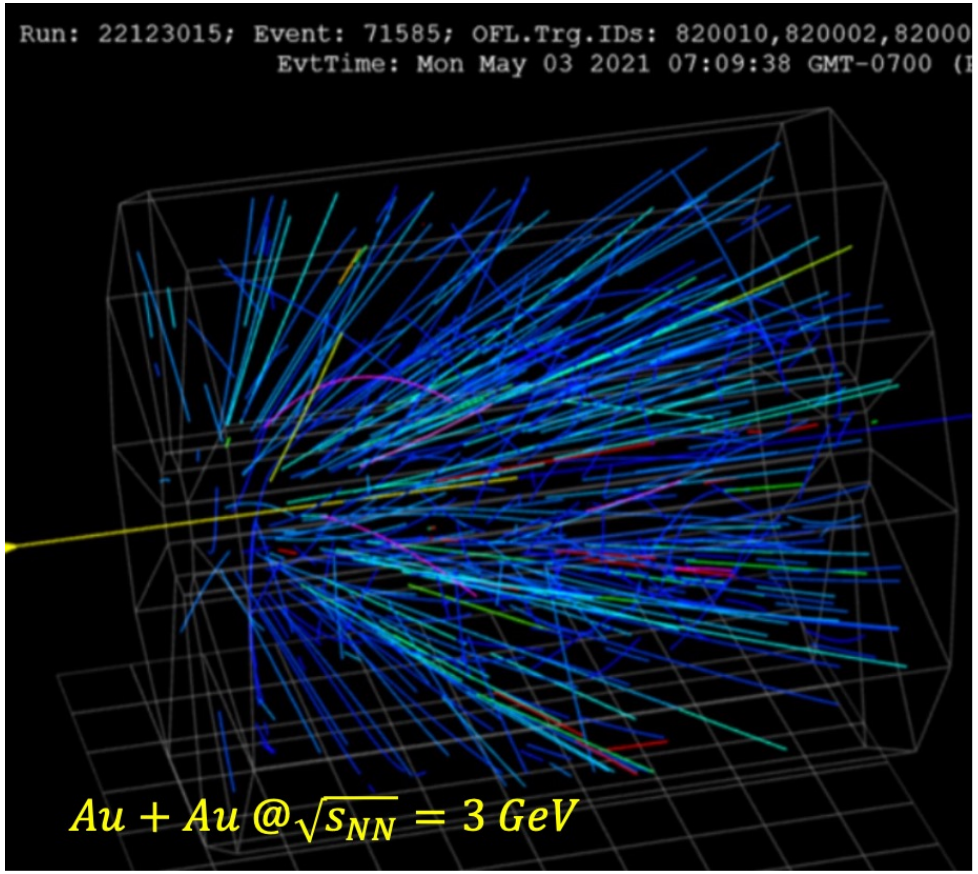

A gold target was installed inside the beam pipe in 2014

Results at 3 GeV from FXT

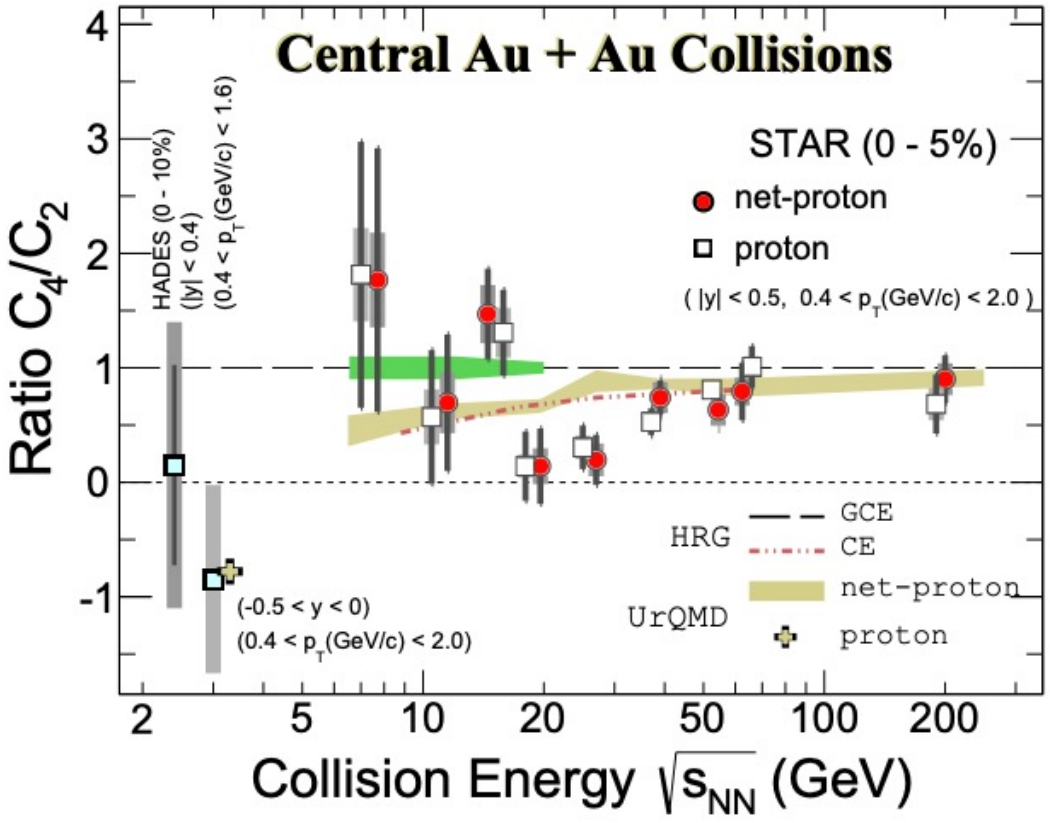

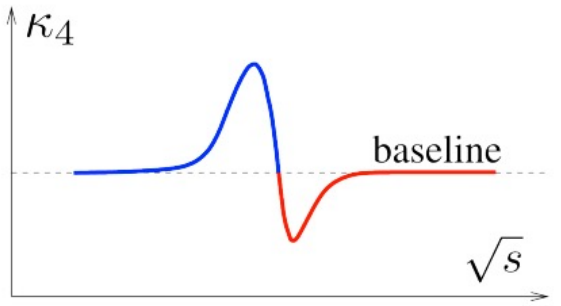

- Non-monotonic energy dependence in central Au+Au collisions (3.1σ)
- Strong suppression in proton C_4/C_2 at 3 GeV
  - *consistent with UrQMD hadronic transport model calculation*

BES-I: PRL 126 (2021) 092301
3 GeV data: PRL 128 (2022) 202303

BES-II data collected at RHIC will cover a broad and interesting range of μ_B for the critical point search

Higher order net-proton number fluctuations

Calculations with a cross-over quark-hadron transition (LQCD and FRG) predict
a particular ordering of susceptibility ratios:

$$\chi_3^B/\chi_1^B > \chi_4^B/\chi_2^B > \chi_5^B/\chi_1^B > \chi_6^B/\chi_2^B$$

PRL 130 (2023) 82301

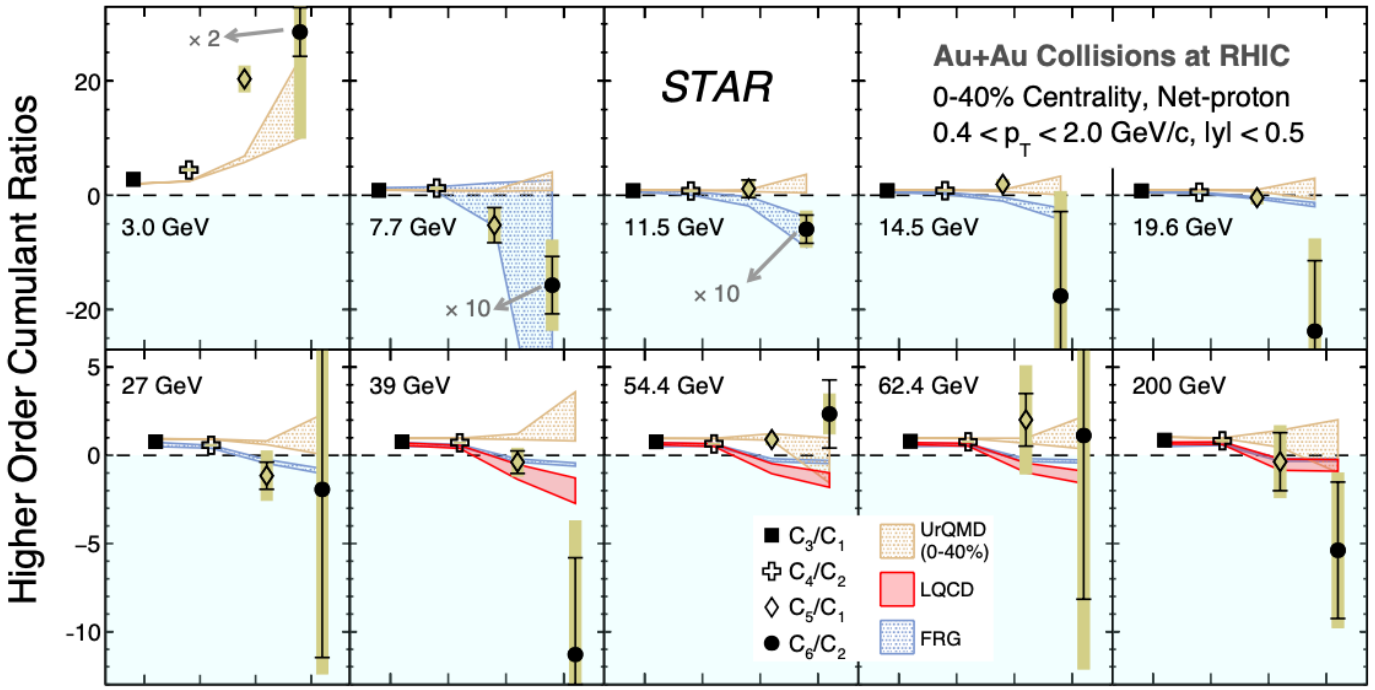

- At 7.7-200 GeV, net-proton cumulant ratios consistent with the ordering predicted by LQCD and FRG:
  $C_3/C_1 > C_4/C_2 > C_5/C_1 > C_6/C_2$
- The 3 GeV data show a reversing trend

The structure of QCD matter at high baryon density μ_B ~720 MeV starkly different from those at vanishing μ_B

Disappearance of partonic collectivity in 3 GeV Au+Au collisions

Phys. Lett. B **827** (2022) 137003

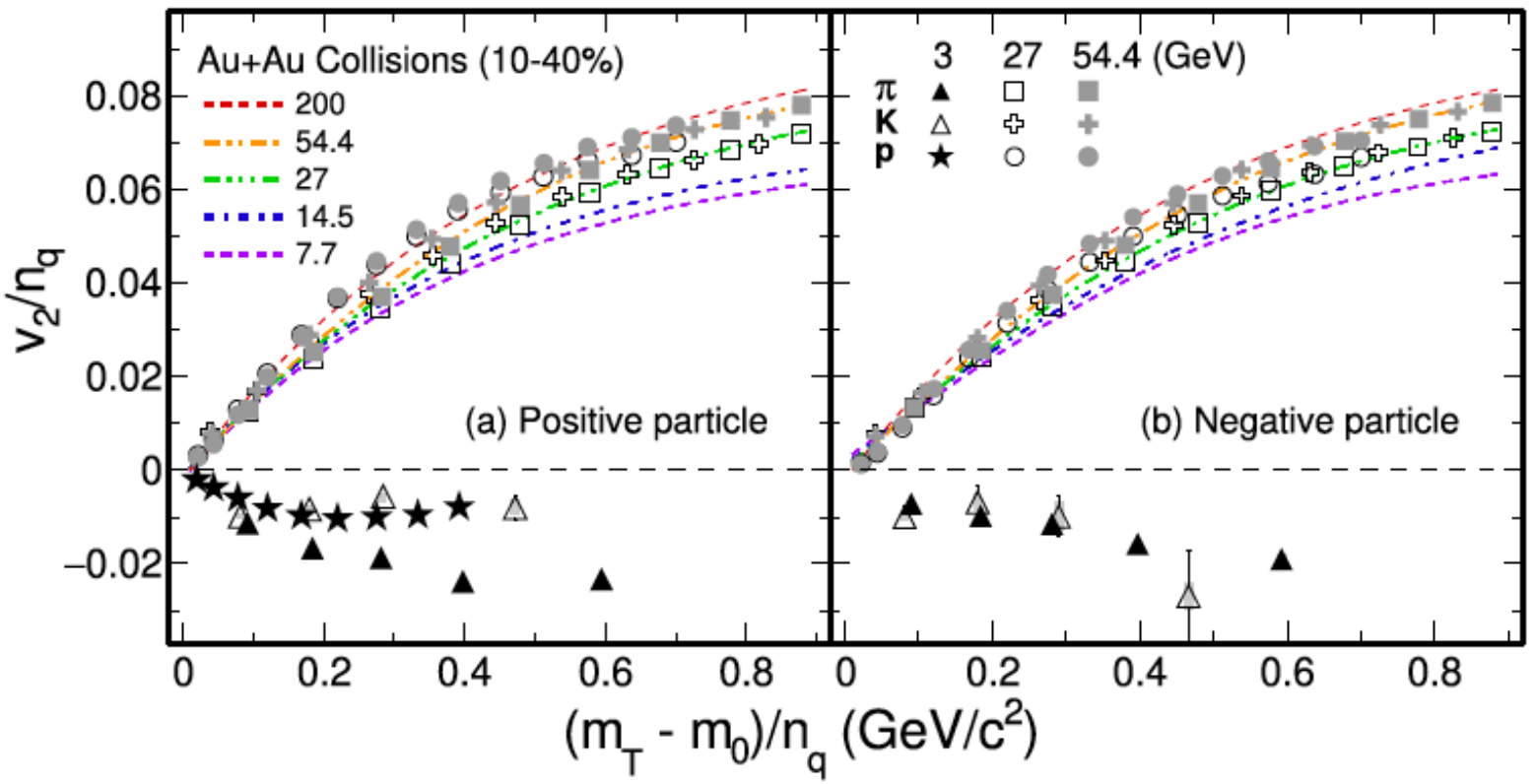

- Number of constituent quark (NCQ) scaling holds at 14.5 GeV and above
- No NCQ scaling and negative elliptic flow observed at 3 GeV

The results can be reproduced with a baryonic mean-field in transport model calculations.

Baryonic interactions dominate in 3 GeV Au+Au collisions

Directed flow of hypernuclei

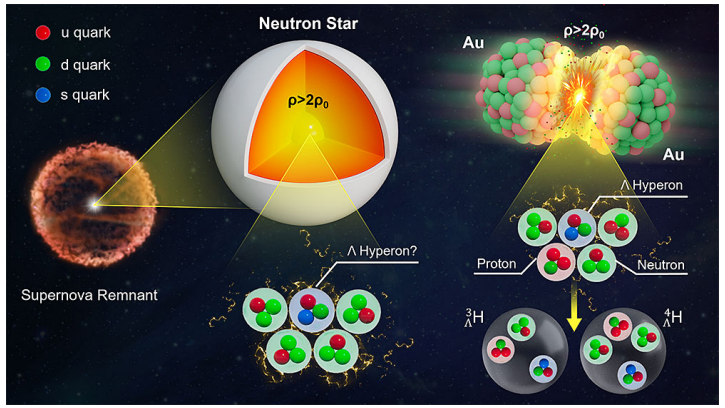

Picture credit:
BNL news article
https://www.bnl.gov/newsroom/news.php?a=121192

Hypernuclei Production

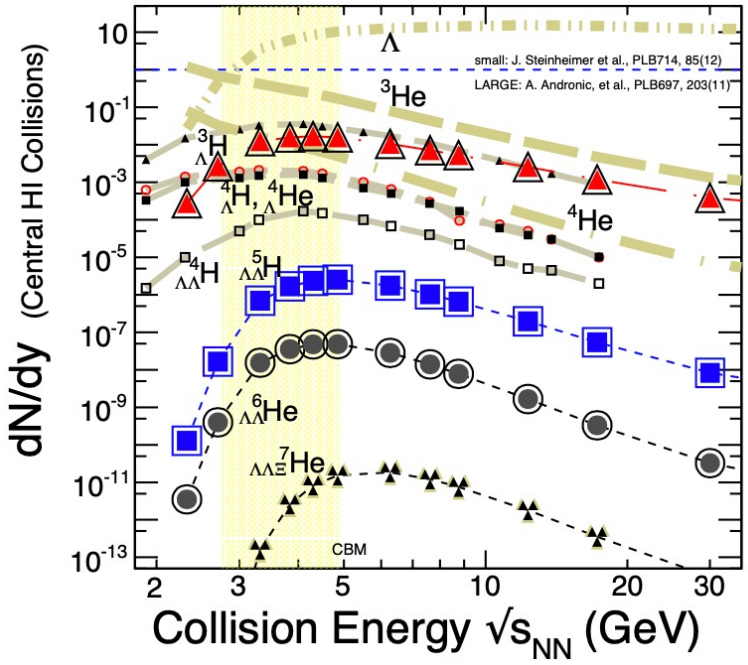

Constrain hyperon – nucleon and hyperon-hyperon interaction
Connection to neutron stars

PRL 130 (2023) 212301

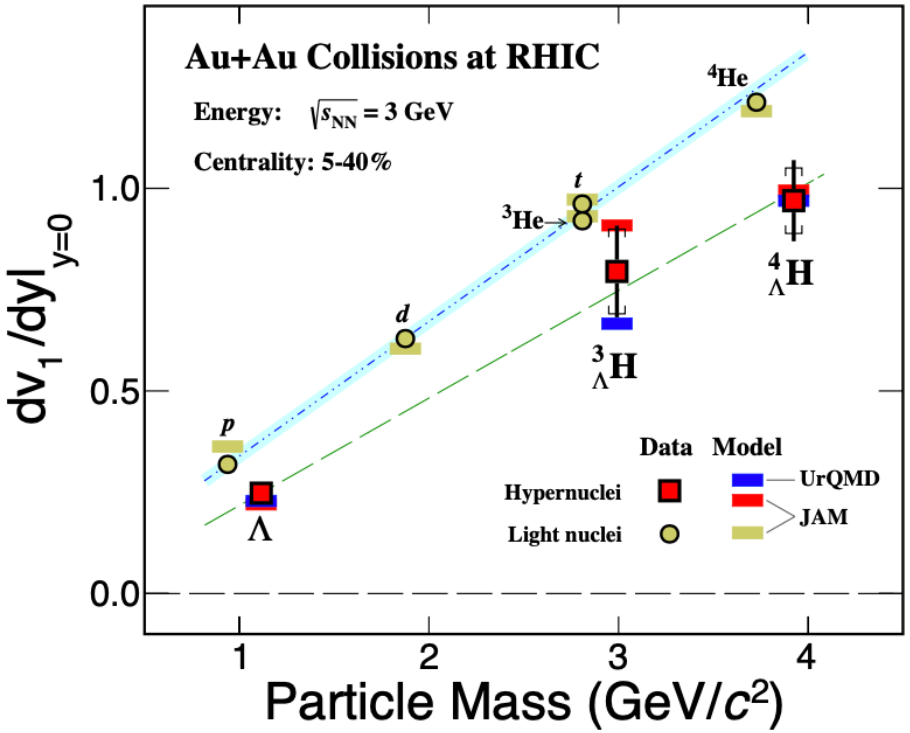

- First observation of significant hypernuclei directed flow in high energy nuclear collisions
- Midrapidity v_1 slopes follow baryon number scaling, implying that coalescence is the dominant production mechanism

Constrain hyperon-nucleon interactions at high baryon density

STAR BES-II upgrades

Major improvements for BES-II

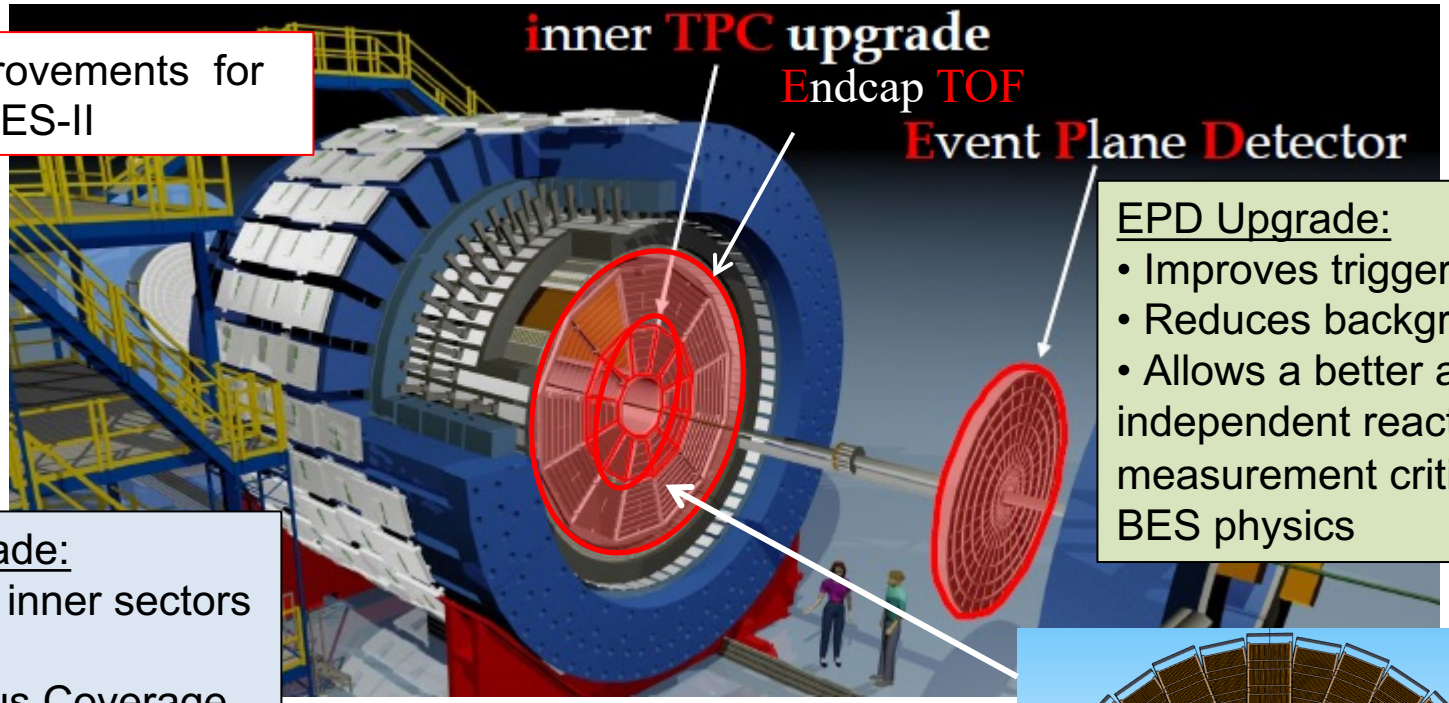

EPD Upgrade:
- Improves trigger
- Reduces background
- Allows a better and independent reaction plane measurement critical to BES physics

iTPC Upgrade:
- Replaced inner sectors of the TPC
- Continuous Coverage
- Improves dE/dx
- Extends η coverage from 1.0 to 1.5
- Lowers p_T cut from 125 MeV/c to 60 MeV/c

EndCap TOF Upgrade:
- Rapidity coverage is critical
- PID at η = 1 to 1.5
- Improves the fixed target program
- Provided by CBM-FAIR

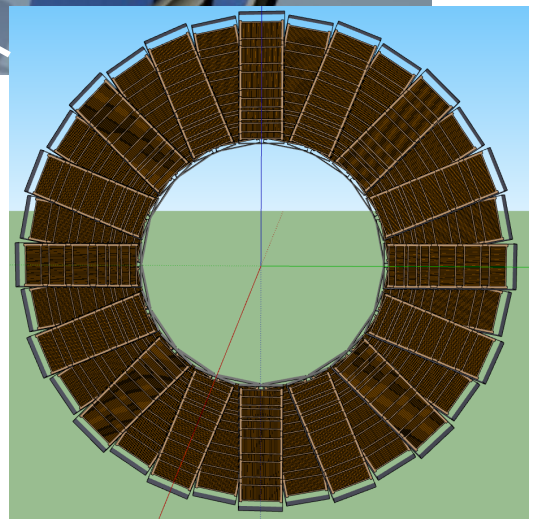

Detector performance

iTPC (2019+)

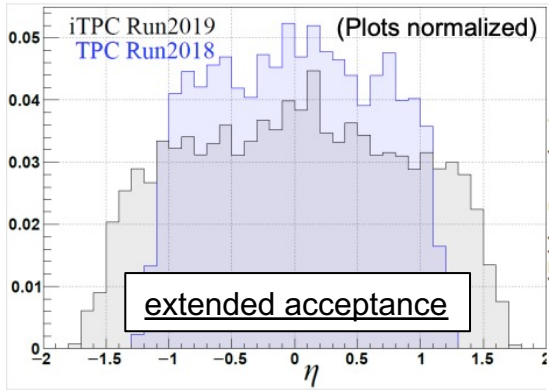

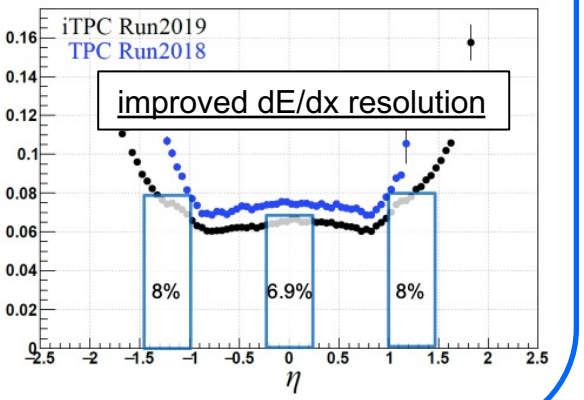

eTOF (2019+)

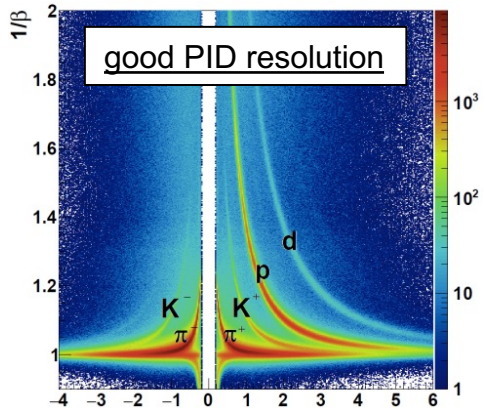

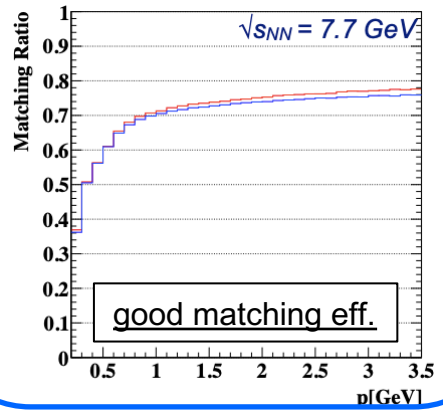

EPD (2018+)

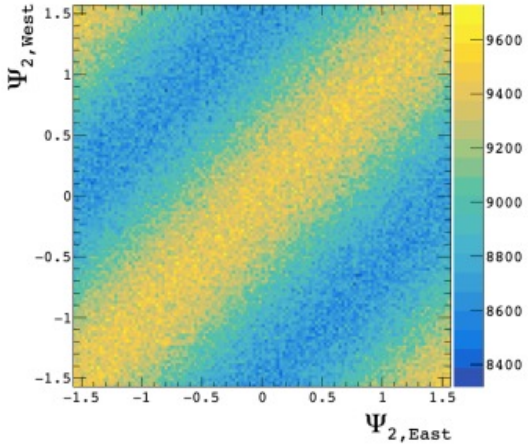

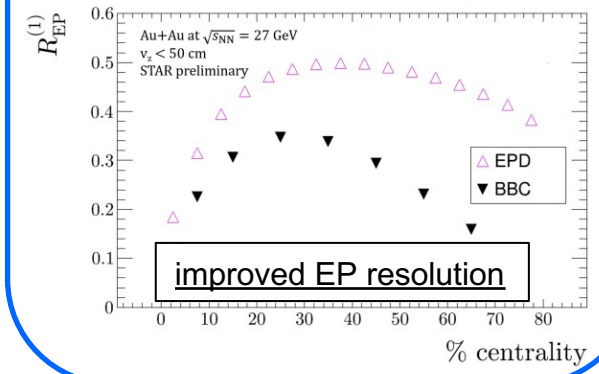

Beam energy scan phase II (BES-II) in 2019-2021

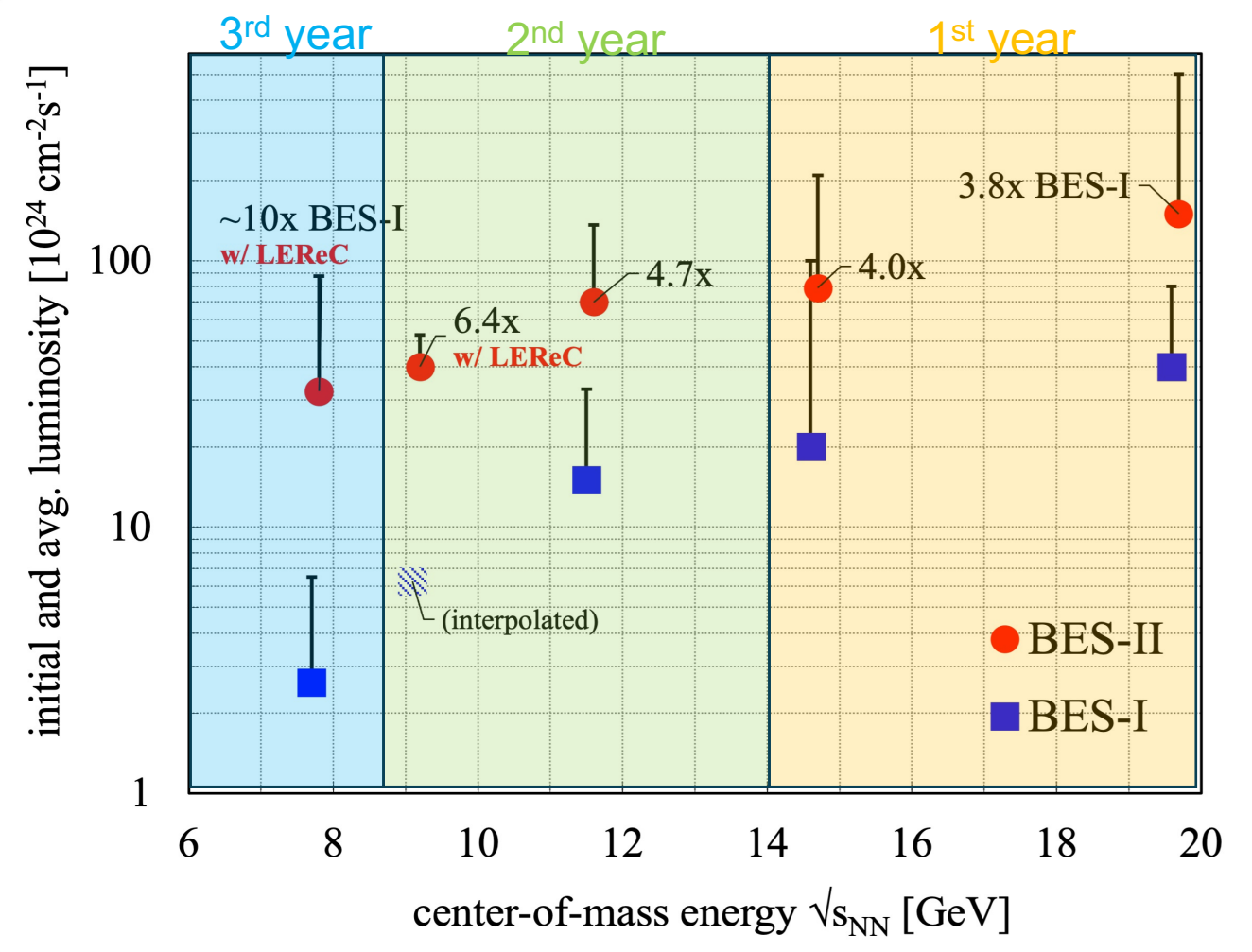

Goal was L_{avg} (BES-II) = 4x L_{avg} (BES-I)

In BES-II

3.8 x L_{avg} (BES-I)
4.0 x L_{avg} (BES-I)

4.7 x L_{avg} (BES-I)
6.4 x L_{avg} (BES-I) ← with LEReC at lowest beam energies

~10 x L_{avg} (BES-I) ←

LEReC: low energy RHIC electron cooling

RHIC is unique to map the phase diagram of QCD:

Beam energy scan II: collision energies 7.7, 9.2, 11.5, 14.6, 17.3, 19.6 GeV and 12 fixed-target energies

In 2021, collected the last collider data set at 7.7 GeV, completed the BES-II program.

BES-II datasets

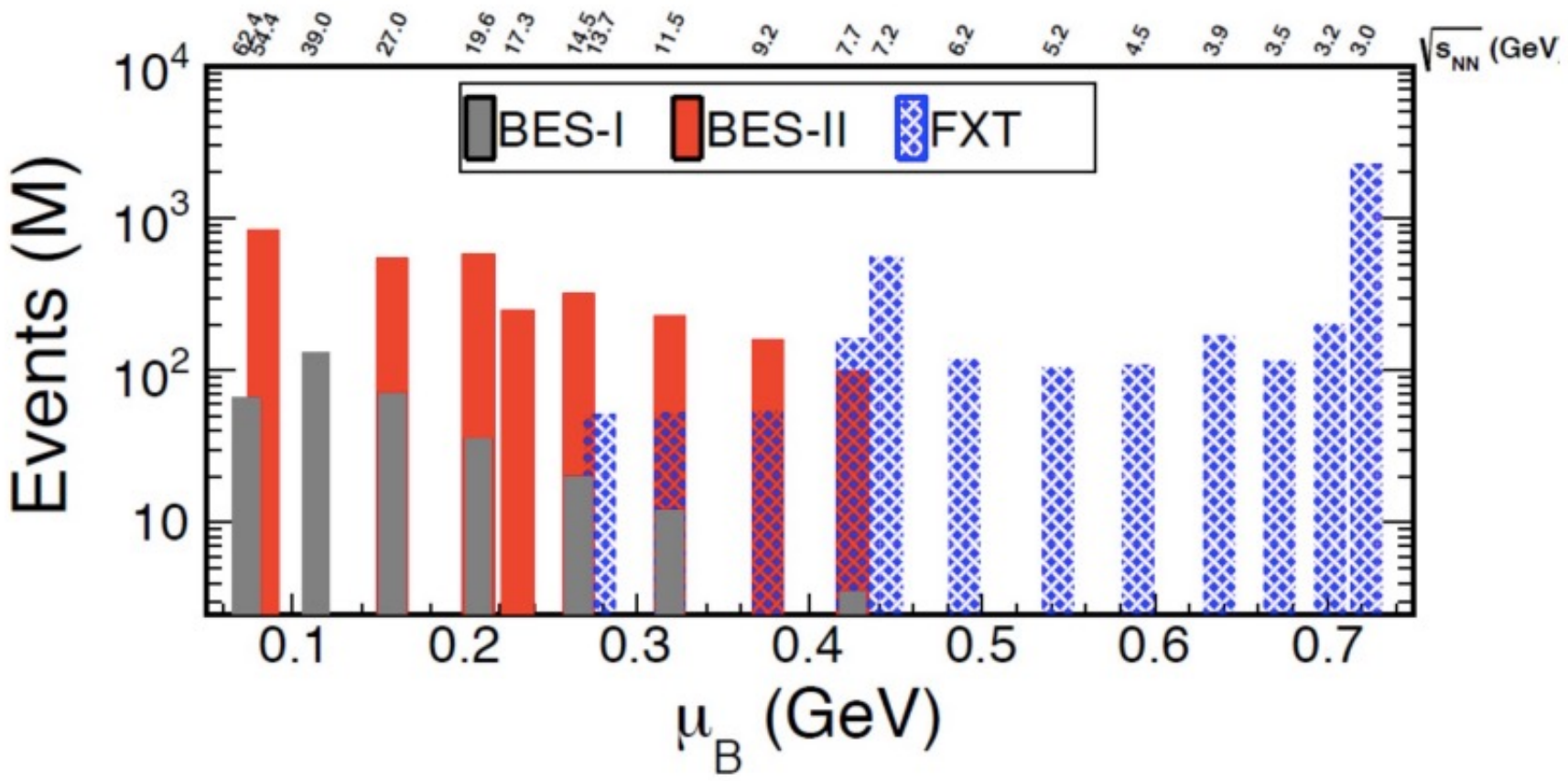

A broad μ_B coverage: $20 < \mu_B < 720$ MeV

BES-II data collected at RHIC will cover a broad and interesting range of μ_B for the critical point search

The phases of QCD matter

The 2023 NSAC Long Range Plan for Nuclear Science

Lattice QCD: crossover chiral transition at $\mu_B < 2$ T

At top RHIC and LHC energies, measurements consistent with a smooth crossover chiral transition

RHIC Beam Energy Scan Phase I (BES-I) measurements imply the QCD critical point, if exists, should be accessible in the center of mass energy region 3-20 GeV

BES-II data taking (energy range 3 - 19.6 GeV) completed in 2021, physics analyses under active pursuit need to be completed

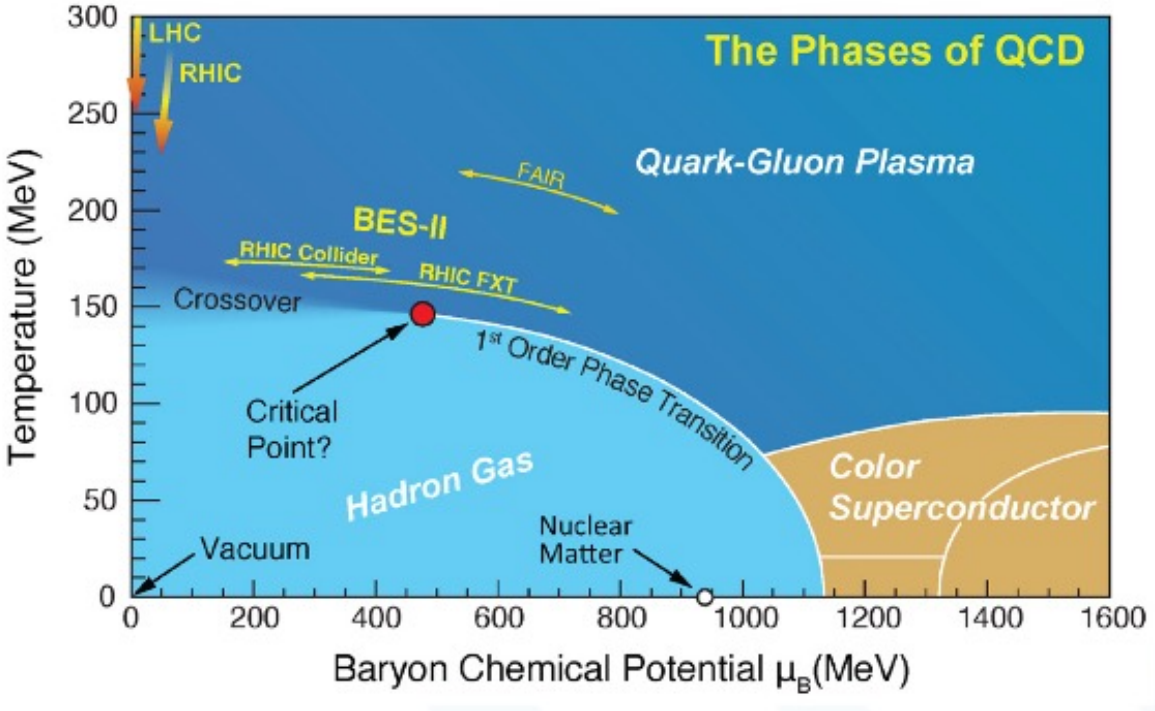

Future experiments, such as CBM at FAIR in Germany will provide additional high statistics and high-resolution data for low-energy collisions and high μ_B

Physics at high baryon density frontier

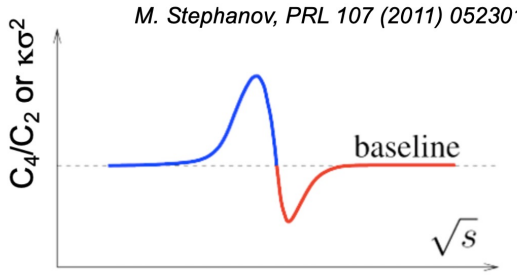

Critical Fluctuations

US-CBM white paper

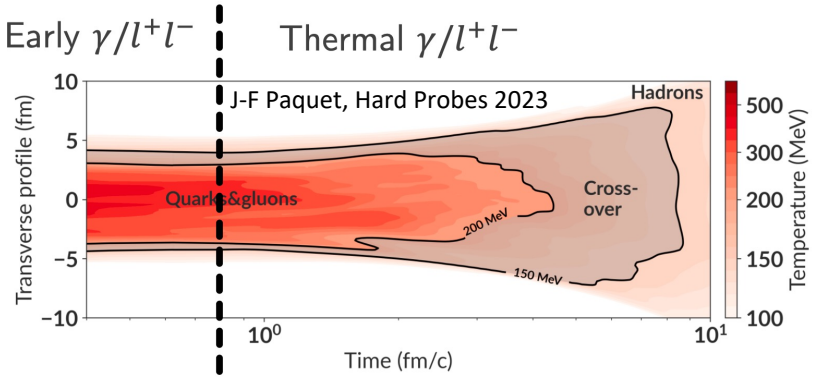

Thermal Radiation

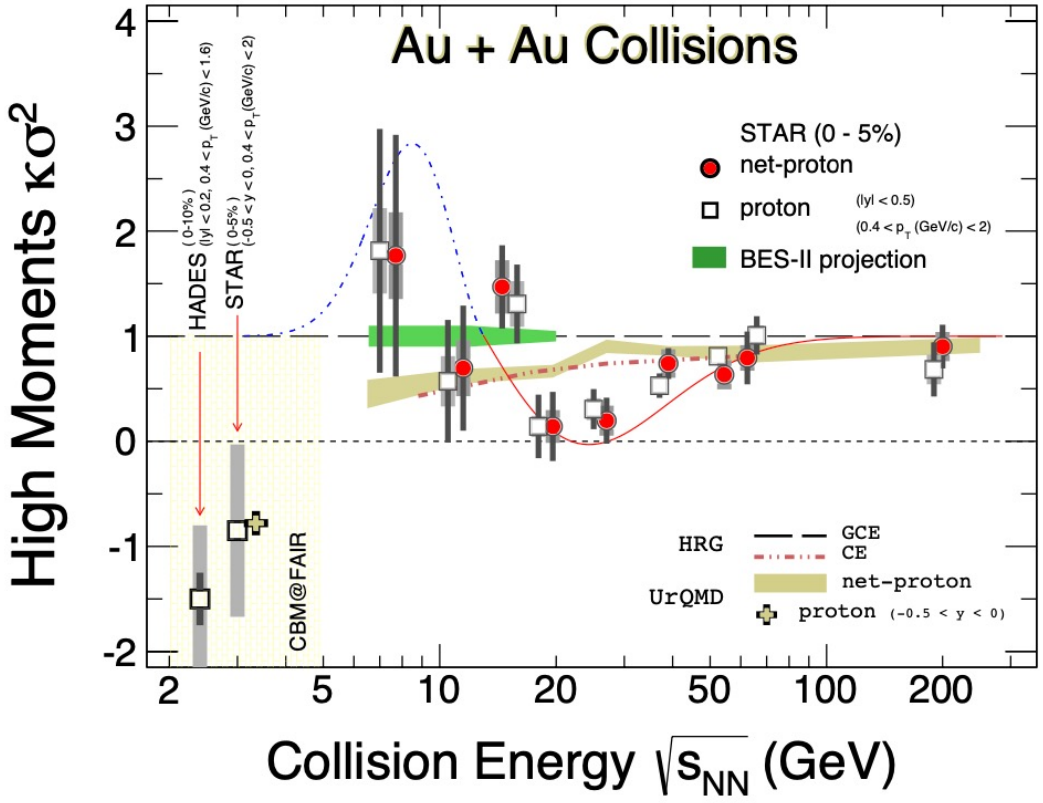

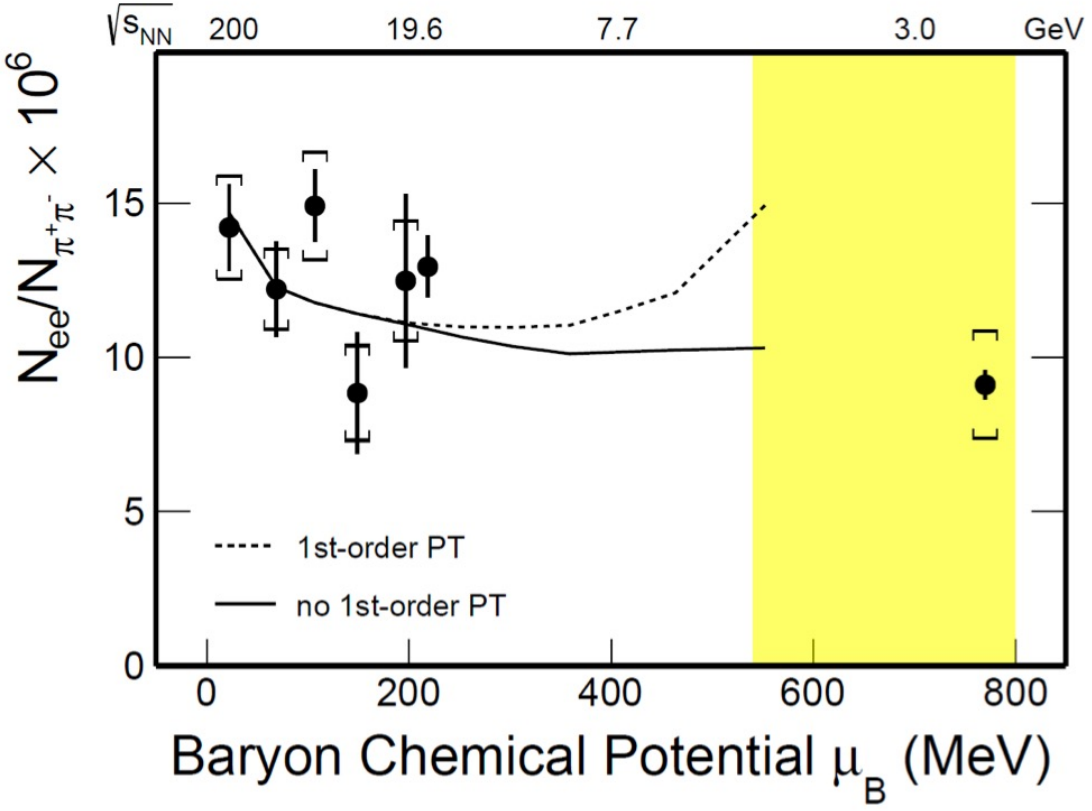

Search for the QCD critical point

Probe first order phase transition

Physics at high baryon density frontier

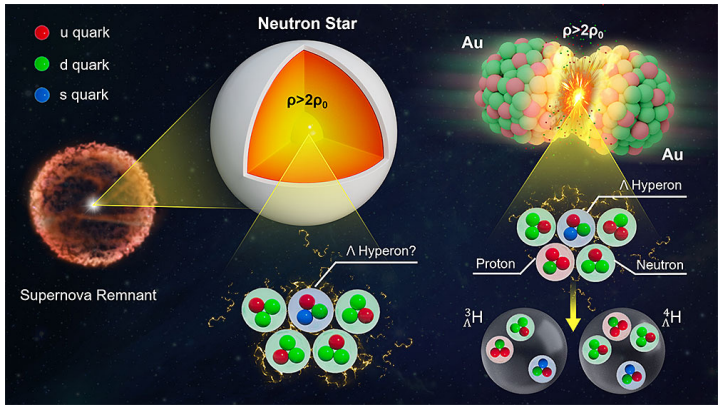

Picture credit:
BNL news article
https://www.bnl.gov/newsroom/news.php?a=121192

Nature 548 (2017) 62

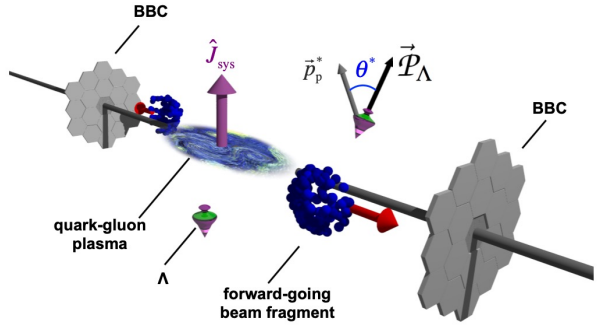

US-CBM white paper

Hypernuclei Production

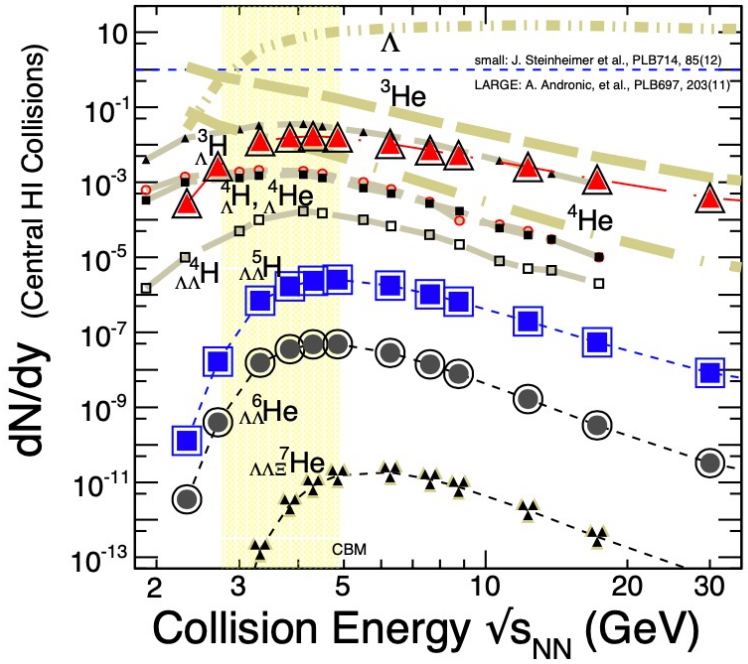

Polarization/Spin Alignment

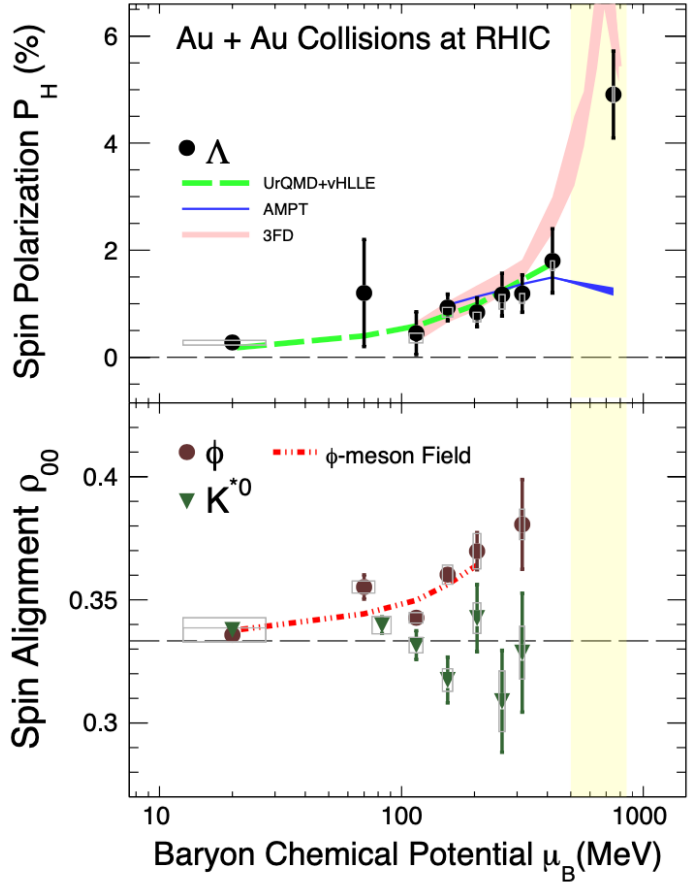

Constrain hyperon – nucleon and hyperon-hyperon interaction
Connection to neutron stars

Probe vorticity field

The future

NA60+ (2029)

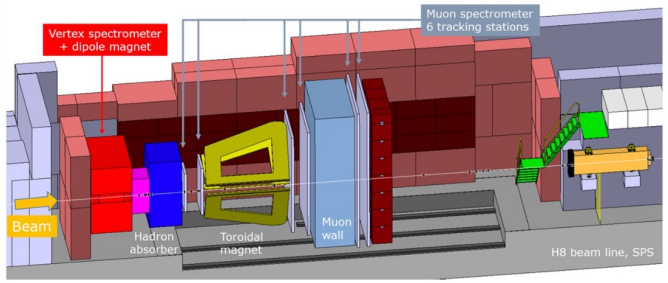

NA61 (2008 - 2027)

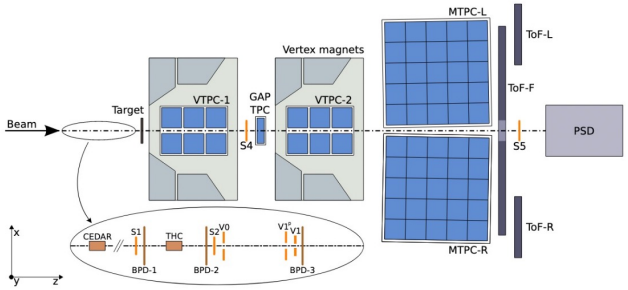

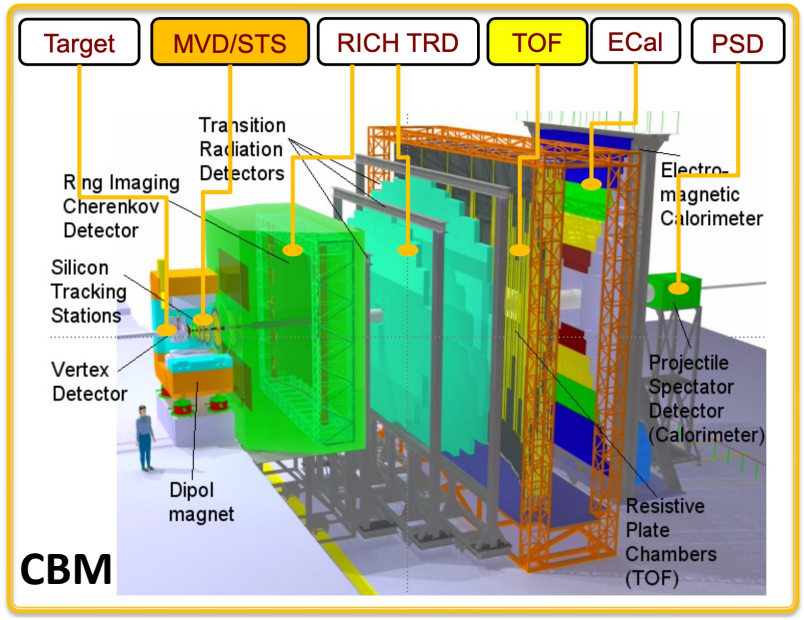

Physics opportunities in the exploration of the QCD phase diagram at high baryon density after the completion of the RHIC BES-II program: NA60+, NA61, CBM, NICA …

Probe the physics of dense baryon-rich matter and constrain the nuclear equation of state in a regime relevant to binary neutron star mergers and supernovae.

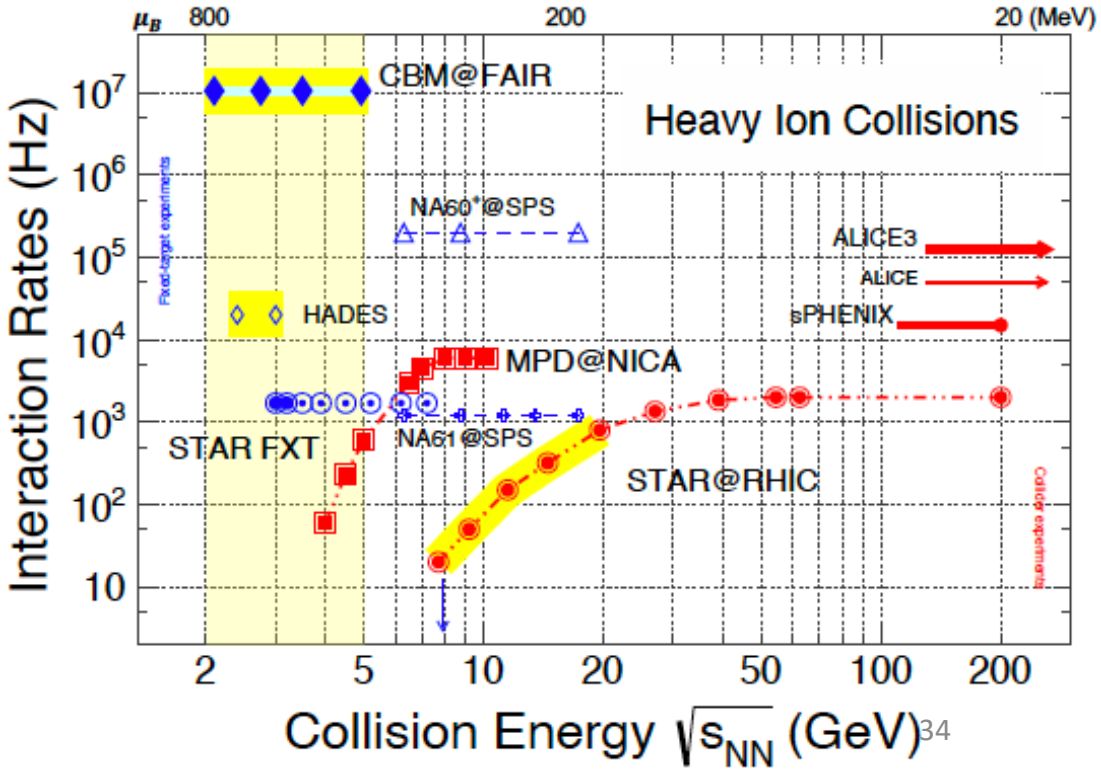

Backup

Identified particle charge-dependent v_1

STAR, arXiv: 2304.03430

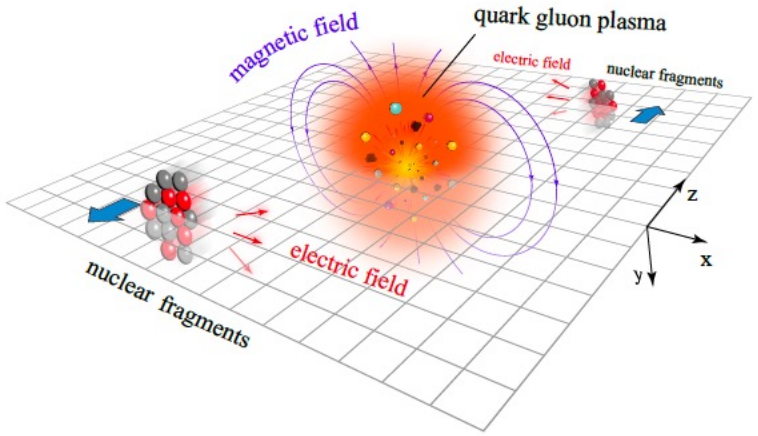

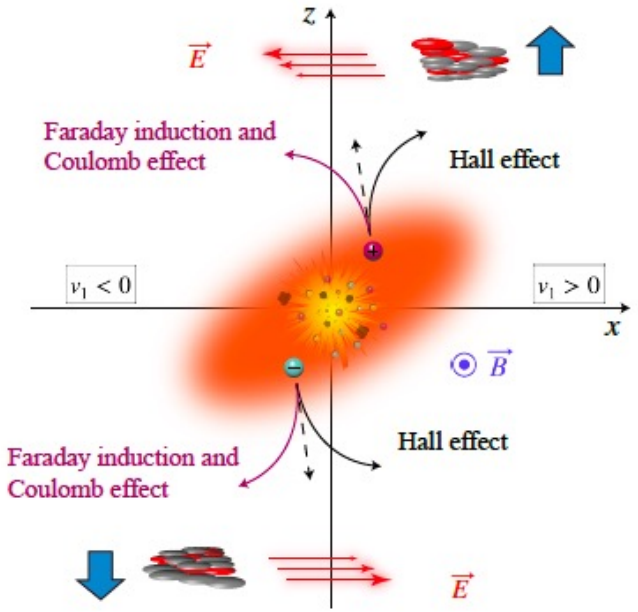

Transported-quark effect:
positive charge-dependent v1 slope

Faraday + Coulomb:
negative charge-dependent v1 slope

Hall effect:
positive charge-dependent v1 slope

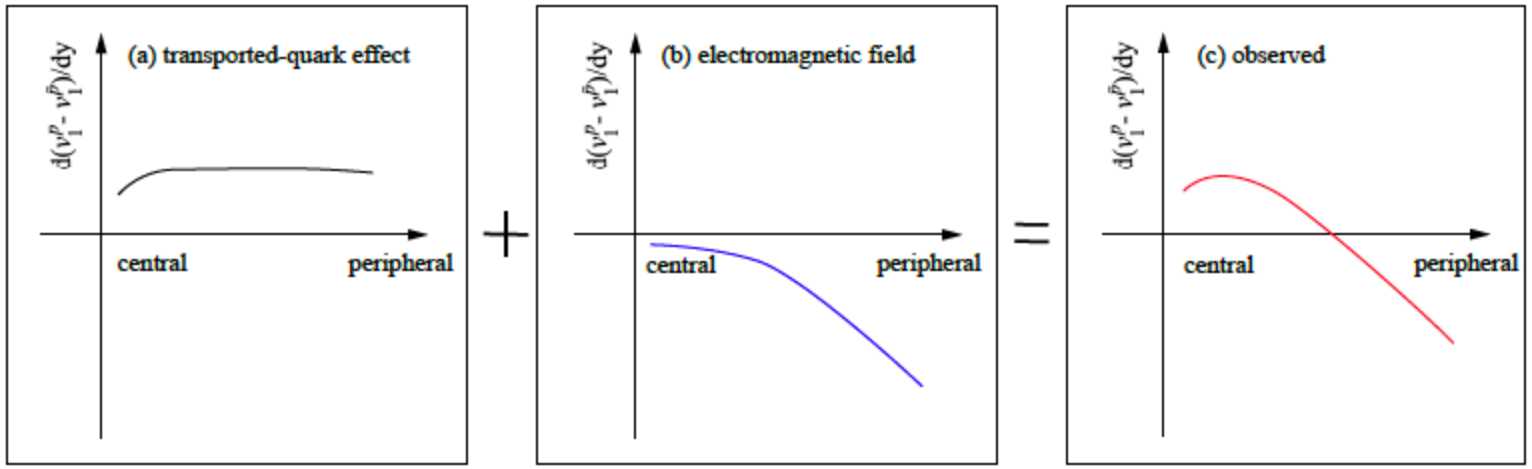

Identified particle charge-dependent v_1

STAR, arXiv: 2304.03430, accepted by PRX

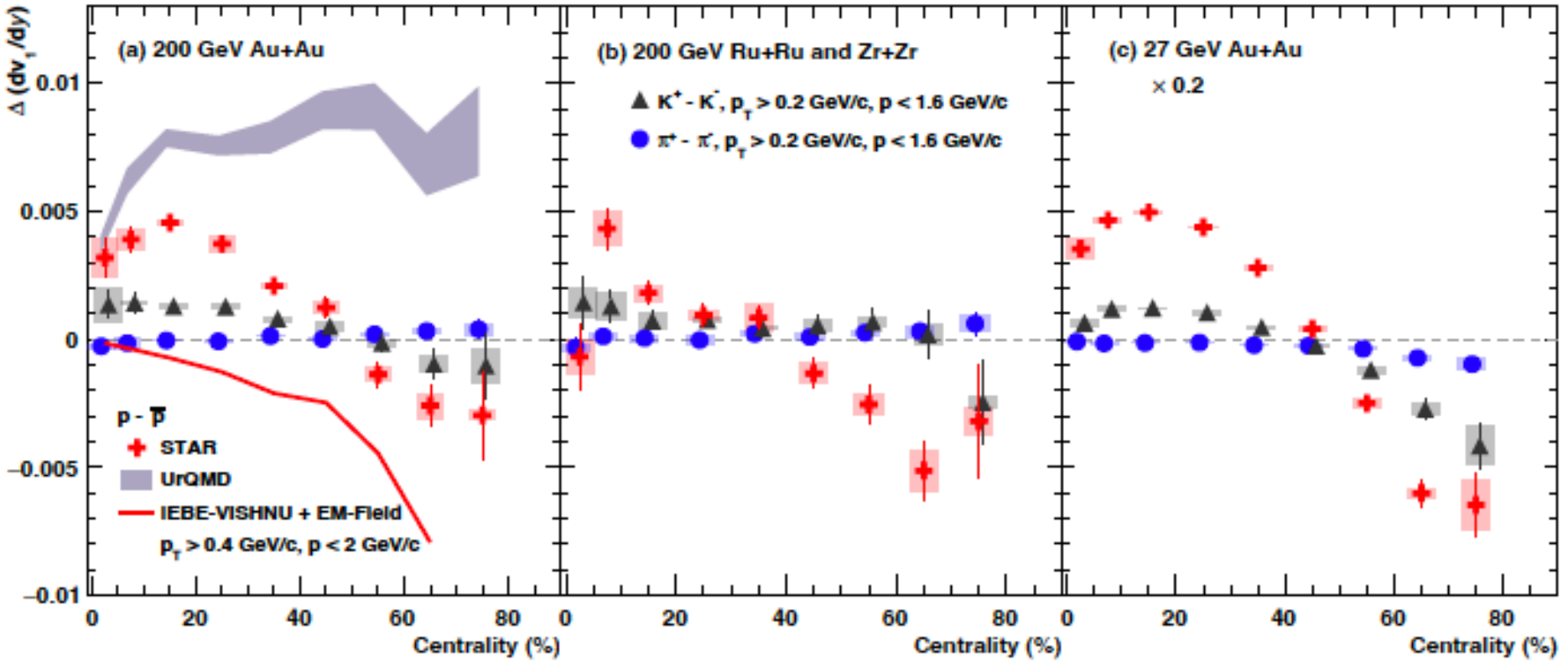

Results in central collisions can be explained by transported quark effect

Results in peripheral collisions consistent with the Faraday induction and Coulomb effect